



RIGA TECHNICAL
UNIVERSITY

Jānis Eidaks

RF POWERING OF AUTONOMOUS WIRELESS SENSOR NETWORK NODES

Summary of the Doctoral Thesis



RTU Press
Riga 2022

RIGA TECHNICAL UNIVERSITY

Faculty of Electronics and Telecommunications

Institute of Radioelectronics

Jānis Eidaks

Doctoral Student of the Study Programme “Electronics”

**RF POWERING OF AUTONOMOUS WIRELESS
SENSOR NETWORK NODES**

Summary of the Doctoral Thesis

Scientific supervisors

Assoc. Professor Dr. sc. Ing.

DMITRIJS PIKULINS

Assoc. Professor Dr. sc. Ing.

ANNA LITVINENKO

RTU Press

Riga 2022

Eidaks, J. RF Powering of Autonomous Wireless
Sensor Network Nodes. Summary of the Doctoral Thesis.

– Rīga: RTU Press, 2022. – 48 p.

Published in accordance with the decision
of the Promotion Council "RTU P-08"
of March 4, 2022, Minutes No. 9.



The research was partially performed within the framework and with the financial support of SAM 8.2.2. "Stiprināt augstākās izglītības institūciju akadēmisko personālu stratēģiskās specializācijas jomās" project of Riga Technical University No. 8.2.2.0/18/A/017.

<https://doi.org/10.7250/9789934227868>
ISBN 978-9934-22-786-8 (pdf)

DOCTORAL THESIS PROPOSED TO RIGA TECHNICAL UNIVERSITY FOR THE PROMOTION TO THE SCIENTIFIC DEGREE OF DOCTOR OF SCIENCE

To be granted the scientific degree of Doctor of Science (Ph. D.), the present Doctoral Thesis has been submitted for the defence at the open meeting of RTU Promotion Council on 10 June 2022 at the Faculty of Electronics and Telecommunications of Riga Technical University, 12 Āzenes Street, Room 201.

OFFICIAL REVIEWERS

Professor Dr. sc. ing. Vjačeslavs Bobrovs
Riga Technical University

Professor Dr.-Ing. habil. Andreas Ahrens
Hochschule Wismar, University of Applied Sciences Technology, Business and Design, Germany

Professor Dr. sc. ing Andrius Katkevičius
Vilnius Gediminas Technical University, Lithuania

DECLARATION OF ACADEMIC INTEGRITY

I hereby declare that the Doctoral Thesis submitted for the review to Riga Technical University for the promotion to the scientific degree of Doctor of Science (Ph. D.) is my own. I confirm that this Doctoral Thesis had not been submitted to any other university for the promotion to a scientific degree.

Janis Eidaks (signature)

Date:

The Doctoral Thesis has been written in English. It consists of an Introduction, 4 chapters, Conclusions, 63 figures, 10 Tables, 3 appendices; the total number of pages is 104, including appendices. The Bibliography contains 91 titles.

Annotation

The work is dedicated to the experimental study of RF powering of autonomous wireless sensor network nodes. The impact of powering signal properties on the RF-DC conversion efficiency and wireless power transfer performance is investigated. The impact of average input power level, peak-to-average power ratio (PAPR) level, different modulation types, signals spectral properties, numbers of sub-carriers, and bandwidth are examined. The most popular RF-DC converter topologies and off the shelf solutions in the sub-GHz frequency range have been studied in detail. The study is performed in four parts: theoretical analysis of WPT technology, RF-DC converter prototyping, experimental study on RF-DC conversion efficiency, and experimental study on WPT performance. The research was partly developed within research projects “Radio Frequency Power Transmission for Wireless Sensor Network Use” and “Advanced Techniques for Wireless Power Transfer” and published in 13 scientific articles.

The Thesis consists of four chapters, 63 figures, 10 tables and 3 appendices. The total number of pages is 85, not including appendices. The Bibliography contains 91 references.

Contents

List of Abbreviations.....	7
Introduction	8
1. Theoretical analysis of WPT technology	13
1.1 WPT techniques	13
1.2. Overview of RF WPT studies	15
1.3 Conclusions on theoretical analysis of WPT technology.....	18
2. RF-DC circuit prototyping	18
2.1 Model development and simulation	18
2.2 Modelling	20
2.3 Rectifier’s input impedance measurements.....	22
2.4 Conclusions on RF-DC circuit prototyping	24
3. Experimental study on RF-DC conversion efficiency	25
3.1 Signal waveform impact on the power conversion efficiency	27
3.1.1 Objective	27
3.1.2 Tasks.....	27
3.1.3 Measurement setup and experiments	27
3.1.4 Experimental results	28
3.1.5 Summary about signal waveform impact on the power conversion efficiency.....	30
3.2 Multitone signal subcarrier number impact on the power conversion efficiency.....	30
3.2.1 Objective	30
3.2.2 Tasks.....	31
3.2.3 Measurement setup.....	31
3.2.4 Experimental results	31
3.2.5 Summary about multitone signal subcarrier number impact on the power conversion efficiency	35
3.3 Matching network impact on the RF-DC conversion efficiency	35
3.3.1 Objective	35
3.3.2 Tasks.....	35
3.3.3 Measurement setup and experiments	35

3.3.4 Experimental results	36
3.3.5 Summary about matching network impact on the RF-DC conversion efficiency	37
3. 4 Conclusions on experimental study on RF-DC conversion efficiency	37
4. Experimental study on WPT performance	38
4.1 Measurement setup.....	38
4.2 Study of the influencing factors on the WPT efficiency.....	39
4.2.1 Signal frequency impact on the WPT efficiency.....	39
4.2.2 Signal waveform impact on the WPT efficiency	40
4.2.3 Constant envelope signal waveform impact on the WPT efficiency	42
4.3 Conclusions on experimental study on WPT performance	43
Conclusions	44
Bibliography.....	Error! Bookmark not defined.

List of Abbreviations

Abbreviation	Explanation
ADS	advanced design system
CHIRP	sweep signal with periodic linearly increasing frequency
DC	direct current
EH	energy harvesting
EM	electromagnetic
EOL	end-of-life
FM	frequency modulation
HBM	harmonic balance method
HPAPR	high PAPR
IFFT	inverse fast Fourier transform
IoT	Internet of Things
LPAPR	low PAPR
NB-IoT	narrow-band Internet of Things
PAPR	peak-to-average power ratio
PCB	printed circuit board
PSMU	power source measure unit
RF	radio-frequency
RPAPR	random PAPR
SDR	software-defined radio
SN	sensor node
USB	universal serial bus
USRP	universal software radio peripheral
VNA	vector network analyzer
WPT	wireless power transfer
WSN	wireless sensor network

Introduction

Relevance

In the last decade, electronic voice assistant devices have been developed to perform tasks directly and control household devices. These and other similar devices are used around us. Some work with the same wireless information transfer protocol and form a wireless sensor network (WSN). The devices that create such networks are called WSN devices. The powering of such WSN devices varies. Some of these devices that serve as a gateway are power-hungry, and some devices consume very little power. The devices occasionally wake to perform some tasks or send data while being in a deep sleep state the rest of the time. Therefore, the operation from the primary power sources – batteries – can be maintained for a long time. However, as the number of such devices is increasing rapidly and generally consumes little power, a more relevant issue is the replacement of the depleted energy source. The battery replacement could be unfeasible if the device is placed in hard-to-reach places or is embedded in the building and has become an integral part of it. The trend of the WSN device use in everyday life is increasing every year, and the devices' convenience is undeniable. Therefore, one of the problems that should be addressed is the sustainable power solution for such devices and prolonging the operation time without expensive and time-consuming battery replacement operations, as the number of such devices is expected only to increase [1].

One of the possibilities of a steerable and controllable energy source is to use wireless power transfer. The wireless power transfer is divided into multiple subtypes, such as electromagnetic (EM) radiation, magnetic resonance, electrical resonance, or electromagnetic induction methods [2], [3]. Of the mentioned methods, the technique that can provide the most considerable WPT distance is the electromagnetic radiation method. Multiple experiments have been performed, and the corresponding scientific papers have been published on the effects of different signal parameters on WPT performance. However, available measurements and the resulting conclusions in some studies are contradictory. They cover only some of the signal parameter impact on the RF-DC power conversion and the converted power from the WPT. Therefore, the research on the signal parameter and waveform impact on the RF-DC power conversion efficiency has yet to be fully explored. There are optimal signal parameters that yield a higher power conversion efficiency with the specified RF-DC converter topology and in the WPT experiments under certain conditions. Therefore, the Thesis is dedicated to the investigation of the signal parameter impact on the RF-DC power conversion and the harvested and converted power with the WPT. As most studies are dedicated to the exploration of RF-DC power conversion with two diode rectifier topologies, this research also reviews this topology.

Research goals and tasks

The main objective of this work is to explore the RF signal parameter impact on the RF-DC power conversion efficiency and the wireless power transfer performance.

The following tasks have been set to reach the defined objective:

1. To develop the RF-DC rectifier models, and provide state-of-the-art analysis and optimisation of the model's parameters.
2. To design and fabricate prototypes for different RF-DC converter solutions.
3. To perform an experimental study on the RF-DC power conversion efficiency of the developed RF-DC converter modules, depending on the RF signal parameters.
4. To perform an experimental study on the wireless power transfer performance of the developed RF-DC converter modules depending on the RF signal parameters.
5. To perform an experimental study on the impact of wireless transmission channels on wireless power transfer performance with different RF-DC power converters.

Scientific novelty and the main results

The results obtained during the investigation are as follows:

- Optimized RF-DC converter models in Advanced Design Simulation (ADS) software have been created.
- The applicability of signals commonly used in communications to efficient RF-DC power conversion and wireless power transfer have been verified.
- RF-DC converter prototypes (voltage doubler topology with matching network, voltage doubler topology without matching network, RF-DC converter based on Powercast P2110B module) have been manufactured.
- A software-defined radio model in MATLAB/SIMULINK environment for RF signal generation has been created. The following signals were implemented:
 - o FM tonal modulation,;
 - o CHIRP;
 - o multitone signal with high PAPR level (same subcarrier amplitudes and phases);
 - o multitone signal with low PAPR level (same subcarrier amplitudes, specifically selected phases);
 - o multitone signal with random PAPR level (subcarrier amplitudes and phases are randomly chosen with the same random seed generator).
- Automated scripts for input signal power level, RF-DC converted DC voltage level measurements in MATLAB/SIMULINK environment, have been created employing selected hardware:
 - o software-defined radio, Ettus USRP B210;
 - o signal generator for specific measurements, Rohde & Schwarz R&S®SMC100A;
 - o digital oscilloscope Tektronix 72004C;
 - o universal power and measurement unit Keysight B2901A.
- Participation in the feasibility study for scientific projects “Radio Frequency Power Transmission for Wireless Sensor Network Use” and “Advanced Techniques for Wireless Power Transfer”.

Theses for defence

In this promotion work, the following theses are proposed and put to defence:

1. The appropriate adjustment of resistance load of the voltage doubler converter to the number of subcarriers, in case of equal synphase multitone signals with uniformly distributed 32–256 subcarriers in the ISM 863–870 MHz frequency range, leads to the maximal RF-DC power conversion efficiency.
2. The exclusion of the matching network for the voltage doubler in the ISM 863–870 MHz frequency range, applying equal synphase multitone signals with uniformly distributed 32–256 subcarriers, increases the RF-DC power conversion efficiency up to 2 times.
3. CHIRP signals, tonally modulated FM, and the amplitude modulated signals with 4–256 subcarriers and PAPR level below 10 dB in the ISM 863–870 MHz frequency range, in case of the voltage doubler converter provides equal power conversion efficiency with the average squared voltage deviation for the converted voltage up to 2.5 %.
4. The application of the CHIRP, FM tonally modulated, and the amplitude modulated signals with 4–256 subcarriers and PAPR level below 10 dB to wireless power transfer and RF-DC conversion with voltage doubler, in the case of the direct line of sight for distance range 1.7–8.7 wavelengths in the ISM 863–870 MHz frequency range, ensures the same WPT performance as a sine signal with the average squared output voltage deviation of 4.5 %.

The research methodology

In order to reach the set goals, the research methodology consists of the current state-of-the-art analysis on the topic, simulation in the ADS environment, the manufacturing of the RF-DC converters, and the measurements of the RF-DC converters depending on various signal parameters.

The literature analysis is focused on 4 RF-DC conversion-related research directions:

- RF-DC power conversion efficiency depending on the signal frequency characteristics;
- RF-DC power conversion efficiency depending on the signal waveforms and envelope type;
- RF-DC power conversion efficiency depending on the input signal power level;
- Different RF-DC power conversion topologies.

The measurements include investigating the different signal parameters (signal input power level, signal bandwidth, number of subcarriers, signal waveform) impact on the power conversion efficiency of the manufactured RF-DC power converters and off-the-shelf available RF-DC power converter module.

The research objects

The research objects in this Thesis are the RF-DC power conversion efficiency and WPT performance of different RF-DC power converter implementations.

Practical application of the research

The results obtained in the experiments show the correlation of impact of different signal parameters on the RF-DC power conversion efficiency and allow the selection of suitable signal parameters to achieve maximum power conversion efficiency and evaluation of the obtained energy using selected RF-DC power converters.

The results of these measurements are included in the feasibility study for scientific projects “Radio Frequency Power Transmission for Wireless Sensor Network Use” and “Advanced Techniques for Wireless Power Transfer”.

Approbation

The results of the research are presented in 13 scientific papers, which have been published in the following conference proceedings and journals:

1. Litvinenko, J. Eidaks, and A. Aboltins, "Usage of Signals with a High PAPR Level for Efficient Wireless Power Transfer," 2018 IEEE 6th Workshop on Advances in Information, Electronic and Electrical Engineering (AIEEE), 2018, pp. 1–5, DOI: 10.1109/AIEEE.2018.8592043.
2. Litvinenko, J. Eidaks, S. Tjukovs, D. Pikulins, and A. Aboltins, "Experimental Study of the Impact of Waveforms on the Efficiency of RF-to-DC Conversion Using a Classical Voltage Doubler Circuit," 2018 Advances in Wireless and Optical Communications (RTUWO), 2018, pp. 257–262, DOI: 10.1109/RTUWO.2018.8587907.
3. S. Tjukovs, J. Eidaks, and D. Pikulins, "Experimental Verification of Wireless Power Transfer Ability to Sustain the Operation of LoRaWAN Based Wireless Sensor Node," 2018 Advances in Wireless and Optical Communications (RTUWO), 2018, pp. 83–88, DOI: 10.1109/RTUWO.2018.8587790.
4. J. Eidaks, A. Litvinenko, A. Aboltins, and D. Pikulins. (2019). Waveform Impact on Wireless Power transfer performance using Low-Power Harvesting Devices. *Electrical, Control and Communication Engineering*, 15(2), 96–103. <https://doi.org/10.2478/ecce-2019-0013>.
5. J. Eidaks, A. Litvinenko, D. Pikulins, and S. Tjukovs, "The Impact of PAPR on the Wireless Power Transfer in IoT Applications," 2019 29th International Conference Radioelektronika (RADIOELEKTRONIKA), 2019, pp. 1–5, DOI: 10.1109/RADIOELEK.2019.8733534.
6. J. Eidaks, A. Litvinenko, J. P. Chiriyankandath, M. A. Varghese, D. D. Shah, and Y. K. T. Prathakota, "Impact of signal waveform on RF-harvesting device performance in wireless sensor network," 2019 IEEE 60th International Scientific Conference on Power and Electrical Engineering of Riga Technical University (RTUCON), 2019, pp. 1–5, DOI: 10.1109/RTUCON48111.2019.8982294.
7. J. Eidaks, A. Litvinenko, A. Aboltins, and D. Pikulins, "Signal Waveform Impact on Efficiency of Low Power Harvesting Devices in WSN," 2019 IEEE Microwave Theory and Techniques in Wireless Communications (MTTW), 2019, pp. 57–61, DOI: 10.1109/MTTW.2019.8897262.

8. S. Tjukovs, A. Litvinenko, D. Pikulins, A. Aboltins, and J. Eidaks, "Waveforms Impact on Performance of Prefabricated Energy Harvesting Device," 2019 IEEE Microwave Theory and Techniques in Wireless Communications (MTTW), 2019, pp. 62–67, DOI: 10.1109/MTTW.2019.8897230.
9. J. Eidaks, J. Sadovskis, A. Litvinenko, and D. Pikulins, "Experimental Analysis of LoRa Signals Employment for RF Energy Harvesting," 2020 IEEE Microwave Theory and Techniques in Wireless Communications (MTTW), 2020, pp. 201–205, DOI: 10.1109/MTTW51045.2020.9245073.
10. Litvinenko, R. Kusnins, A. Aboltins, J. Eidaks, D. Laksis, and J. Sadovskis, "About Simultaneous Information and Power Transfer in WSN using Frequency Modulation," 2020 IEEE 8th Workshop on Advances in Information, Electronic and Electrical Engineering (AIEEE), 2021, pp. 1–6, DOI: 10.1109/AIEEE51419.2021.9435778.
11. Eidaks, J., Kušņins, R., Laksis, D., Babajans, R., Litviņenko, A. "Signal Waveform Impact on RF-DC Conversion Efficiency for Different Energy Harvesting Circuits". 2021 IEEE Workshop on Microwave Theory and Techniques in Wireless Communications (MTTW 2021): Conference Proceedings, Latvia, Riga, 7–8 October 2021. Piscataway: IEEE, 2021, pp.1–6. ISBN 978-1-6654-2470-7. e-ISBN 978-1-6654-2469-1. Available from: DOI:10.1109/MTTW53539.2021.9607090
12. Eidaks, J., Kušņins, R., Babajans, R., Čirjuļina, D., Semeņako, J., Litviņenko, A. "Fast and Accurate Approach to RF-DC Conversion Efficiency Estimation for Multi-Tone Signals". Sensors, 2022, Vol. 22, No. 3, Article number 787. ISSN 1424-8220. Available from: DOI:10.3390/s22030787
13. Kušņins, R., Babajans, R., Eidaks, J., Čirjuļina, D., Litviņenko, A. " Performance Estimation for RF Wireless Power Transfer Under Real-Life Scenario " 2022 IEEE 21st Mediterranean Electrotechnical Conference (MELECON). Submitted.

The author of the Thesis has presented the research results at the following international scientific conferences:

1. "2018 IEEE 6th Workshop on Advances in Information, Electronic and Electrical Engineering (AIEEE)", Lithuania, Vilnius, 8–10 November 2018.
2. Riga Technical University 60th International Scientific conference (Section electronics), Latvia, Riga, 26 April 2019.
3. "29th International Conference Radioelektronika 2019", Czech Republic, Pardubice, 16–18 April 2019.
4. "MTTW 2019: IEEE Workshop on Microwave Theory and Techniques in Wireless Communications 2019", Latvia, Riga, 1–2. October 2019.
5. "2019 IEEE 60th International Scientific Conference on Power and Electrical Engineering of Riga Technical University (RTUCON)", Latvia, Riga, 7–9 October 2019.
6. "MTTW 2020: IEEE Workshop on Microwave Theory and Techniques in Wireless Communications 2020", Latvia, Riga, 1–2 October 2020.

7. “2021 IEEE 6th Workshop on Advances in Information, Electronic and Electrical Engineering (AIEEE)”, Lithuania, Vilnius, 22–24 April 2021.

Thesis structure

The Thesis consists of an introduction, four chapters, conclusions, and 3 annexes, with a total number of pages 104.

The Introduction is dedicated to setting the goals and tasks required to achieve the research objective, the proposed theses, and the possible application of the achieved results.

Chapter 1 is dedicated to a short theoretical overview of the WPT technology.

Chapter 2 is dedicated to the RF-DC converter parameter modelling and detection of the converter’s optimal parameters for achieving the maximum power conversion efficiency impacted by the converter’s component values.

Chapter 3 is devoted to the investigation of the impact of different signal parameters on the RF-DC converter performance. This research direction is further divided into several sub-topics:

- impact of the signal waveform on the power conversion efficiency;
- impact of the number of the multitone signal subcarriers on the power conversion efficiency;
- impact of the matching network on the RF-DC conversion efficiency;
- impact of the signal waveform on the WPT performance.

Chapter 4 is dedicated to the study of wireless power transfer and the impact of the channel and different signal waveforms on its performance. In this study, various rectifier boards are used, and the received WPT RF signal average input power and converted RF-DC power are analysed.

The Conclusions are summarising the RF-DC and WPT performance results and the corresponding trends observed from the experiments.

1. Theoretical analysis of WPT technology

One of the solutions to provide energy to the WSN nodes over the distance independently of the environment conditions is to employ wireless power transfer (WPT). This solution enables to provide the WSN nodes with a steady supply of energy and eliminates the use of batteries – therefore, also battery recycling. Depending on the conditions and the placement of the WSN nodes, under specified conditions, it is also possible for the WSN node to use ambient RF signal harvesting.

1.1. WPT techniques

The frequency range of the signal employed for the RF energy harvesting in the form of an electromagnetic radiation is 3 kHz to 300 GHz [4]. The RF energy transfer and harvesting can be divided into multiple groups depending on the properties, i.e., it can be characterized depending on the field region:

1. Near field region, where the systems load impedance of the receiver's sides affects the load impedance of the transmitter's sides [3], which can be classified into two groups:
 - a) inductive power transfer and magnetically coupled resonance WPT, where the energy is transferred using the magnetic field generated from the current flowing through the transmitter coil to the receiver coil [5];
 - b) capacitive power transfer, where the energy is transferred through the so-called displacement current through the capacitors [3], [5].
2. The far-field region, where the system's load impedance of the receiver's sides does not affect the load impedance of the transmitter's sides [3], electromagnetic radiative radiation.

The efficiency of the near-field WPT systems can reach more than 90 % with the distances between the transmitter and receiver from a few millimetres up to few centimetres [5]. The efficiency of the far-field WPT systems achieves much lower power conversion efficiency and is dependent on the distance, the antenna gains, and the transmitter power level. Due to the limited distance that the near field WPT systems can power the receiver side, these systems will not be reviewed further. Therefore, the WPT system, which employs electromagnetic radiation for energy transfer, will be reviewed. The WPT system block diagram is shown in Fig 1.1.



Fig. 1.1. The block diagram of the WPT system.

The WPT system consists of 3 different power conversion subsystems: energy transmitter, wireless channel, and energy receiver. In this system, power conversion is implemented as follows:

- the DC power is converted to the RF signal power, where the conversion efficiency is defined as η_1 ;
- the RF power is further transferred to the wireless channel and received at the energy receiver; this conversion efficiency is denoted as η_2 ;
- finally, the received RF power is converted from the RF signal to the DC power, characterized by another conversion efficiency η_3 .

$$\eta_{II} = \eta_1 \cdot \eta_2 \cdot \eta_3 \quad (1.1)$$

The overall efficiency of WPT can be expressed with the efficiencies of these three main components:

$$\eta_1 = \frac{\overline{P}_{RF}^{Tx}}{\overline{P}_{DC}^{Tx}}, \eta_2 = \frac{\overline{P}_{RF}^{Rx}}{\overline{P}_{RF}^{Tx}}, \eta_3 = \frac{\overline{P}_{DC}^{Rx}}{\overline{P}_{RF}^{Rx}}, \quad (1.2)$$

where η_{II} – total efficiency of the WPT system; η_1 is efficiency of the transmitter; η_2 is efficiency of the wireless channel; and η_3 is efficiency of the receiver.

Equations (1.1) and (1.2), and Fig. 1.1 show that maximizing of the total efficiency η_{II} requires maximizing of η_1 , η_2 , and η_3 combined, as the total efficiency depends on them.

1.2. Overview of RF WPT studies

For the WPT and energy harvesting, one of the most important parts is the rectifier in conjunction with antenna, also called rectenna. The function of the rectenna is to convert the RF power signal to DC voltage for low power sensors and/or DC/DC converters for additional voltage boosting for sensors that require higher DC voltage. The performance of the rectenna and the distance between the transmitter and rectenna will also impact the converted power level and will affect the operation of the device. To perform efficient energy transfer or to create an accurate WPT model for the rectenna, of the following considerations must be taken into account:

- the topology of RF-DC converter;
- signal frequency;
- signal waveform;
- input power level.

The key properties of the proposed rectennas ordered by frequencies and input powers as well as topology, powering signals, and obtained conversion efficiency are summarized in Table 1.1 [6]. Multiple RF-DC rectenna measurements with the specified topology show a very high-power conversion efficiency, above 70 % with a relatively high input power level above 15 dBm [8]–[12], [22]–[16]. In order to achieve such input power level at the RF-DC rectifier input, the transmitter side should generate a power level of two to three magnitudes higher, and even more, if the distance is increased, it would exceed the allowed specified effective isotropic radiated power (E.I.R.P.).

Some of the RF-DC topologies [8], [11] optimized for high input power level operation with GaAs diodes as rectifier diodes manage to achieve the power conversion efficiency that exceeds 90 %. However, the specified input power level is not suitable for use in WSN nodes, as the transmitter E.I.R.P. exceeds the transmitter power regulation limit.

The use of input power in the range around 0 dBm implies the application of both SN and low-power technologies, such as RFID and E-ink [23], [24]. This range of input RF power was less frequently addressed in literature than high and low ($\ll -15$ dBm) power ranges. Comparing rectennas in terms of frequency, Table 1.1 demonstrates that rectennas were mainly developed for the 2.45 GHz ISM frequency band. The use of high frequency also limits the effective distance between the transmitter and the SN. Sub-GHz ranges, such as 433 MHz (ISM) and 860 MHz (GSM-850), allow power transfer to greater distances [6].

Most of the reviewed studies use the sine wave signal as the input signal for the RF-DC rectifiers. However, some of the studies, such as [17], [21], [22], [25]–[29], revealed that the power conversion with the multitone signal yielded a higher percentage of efficiency than with the sine wave.

Table 1.1
Comparison of Different RF-DC Rectifier Topologies [6]

Ref.	Substrate	RF-DC	Frequency, GHz	RF Input Power, dBm	Waveform	PCE, %
		Topology				
[7]	-	1 diode	24	27	Single-tone ¹	43.6
				16		42.9
[8]	Custom ³	4 diodes	5.8	30	Single-tone	92.8
[9]	FR4	2 diodes	5.76	20	Single-tone	84
[10]	RT/Duroid 5870	1 diode	5.8	16.9	Single-tone	82.7
			2.45	19.5		84.4
[11]	Custom ⁴	1 diode	2.45	37	Single-tone	91
[12]	FR4	2 diodes	2.45	24.7	Single-tone	78
[13]	RO4003C	1 diode	2.45	3	Multi-tone ²	54.5
[14]	FR4	4 diodes	2.4	27	Multi-tone	75
[15]	PTFE	4 diodes	2.4	26.2	Single-tone	80
[16]	FR4	2 diodes	2.4	22	Single-tone	82.3
[14]	RO4003C	1 diode	2.4	10	Single-tone	60
[17]	-	1 diode	2.4	-10	Multi-tone	42
[18]	FR4	4 diodes	2.15	0	Single-tone	70
[19]	Arlon A25N	1 diode	0.915	0	Multi-tone	67.8
[20]	RT/Duroid 5880	2 diodes	0.86	-4	Single-tone	60
[21]	-	1 diode	0.433	-10	Multi-tone	55

¹ All instances of “single-tone” refer to an unmodulated carrier.

² All instances of “multi-tone” refer to a sum of several subcarriers.

³ Relative permittivity $\epsilon_r = 3.4$, the dielectric loss tangent $\tan\delta = 0.0015$.

⁴ Relative permittivity $\epsilon_r = 2.55$, the dielectric loss tangent $\tan\delta = 0.0018$ [6].

The topology of the RF-DC circuit is another crucial parameter of rectenna design. The topologies of the reviewed scientific papers revealed the most used topologies: one-diode-based (half-wave rectifier), two-diode-based (voltage doubler), and four-diode-based (diode bridge

rectifier) topologies. These topologies with slight variations were used in the studies listed in Table 1.1. After reviewing the power conversion efficiency performance of the rectifiers shown in Table 1.1 [6], it can be concluded that a rectenna based on a voltage doubler RF-DC converter working at a sub-GHz frequency and multi-tone power-carrying signals proved to be the most well-balanced solution in terms of cost and efficiency for RF WPT applications targeted at powering SN and low power electronics [6].

The studies reviewed were mainly focused on improving the performance of rectennas with experimental verification of the results to develop robust theoretical models for WPT and RF-DC converters. In the field of AC-DC [30] and DC-DC [31], [32] converters, various theoretical models have been developed. Several modelling approaches have also been proposed for RF-DC circuit precise simulations. Developing an accurate simulation model is a feasible alternative to experimental studies of RF-DC power converters, proposing a more convenient and cost-effective methodology, not requiring the fabrication of physical prototypes, especially when circuit design optimization is required.

The comprehensive analysis of non-linear circuits not amenable to linearization is usually a time-consuming and complicated task, despite recent advances. The application of complex input signals makes the issue even more pronounced. The inherent long transients of RF-DC converters make one of the most robust circuit analysis methods – transient analysis (TA) [33] – unsuitable due to disproportionately long simulation times [34]. Furthermore, a vast number of iterations is required in the case of narrow-band signals with periodic envelopes, as the simulation step must be much smaller in comparison to the period of the carrier wave. Despite the study results on speeding up the TA [35], the mentioned restriction on the simulation step size intrinsically limits the method's performance. The Volterra series method [36] is another widely used non-linear circuit analysis methodology. The method's main disadvantage is a prolonged convergence rate for circuits with highly pronounced non-linearity. The harmonic balance (HB) method was initially proposed in [37] to solve problems in mechanical engineering. Subsequently, it has been adapted to deal with various non-linear circuits under sinusoidal excitation [38]. The HB method allows computing the steady state response directly, involving solving a system of non-linear equations [39], thus eliminating the issue of significant transient times. Another approach is based on the preliminary partitioning of the original system into linear and non-linear parts [40]. The resulting non-linear equations can be solved, e.g., utilizing Newton's method (NM) [41] or iteration relaxation method (IRM) [42], [43]. It has been shown that the evaluation of the Jacobian matrix for NM can be significantly accelerated using FFT algorithms [44]. The convergence at high input power levels could be ensured through the continuation method [45]. The multi-tone input signals could be handled by employing a modified HB [46], [47]. However, a significant rise in computational burden is observed due to the necessity of calculating large Jacobian matrixes.

Despite the methods' accuracy, their application is still resource and time-demanding. This led to the development of approximate closed-form expression-based models, applied to the analysis of rectennas sharing a common load [48], single diode rectifiers [49], [50], and Class F rectifier converters. The simulations of the SPICE model, based on the parameters obtained from experimental data through curve fitting, demonstrated the PCE up to 90 % for the input

power range of 30–35 dBm at 2.4 GHz [11]. Comparable results have been obtained in [51] for a single diode rectifier using an analytical model, including the transmission line effect. An approximate model was used in [52] to find PCE for multi-tone excitation with equally spaced frequencies. It has been proven that most analytical models, not taking into account the nonlinearity of the diodes and the possible influence of the PCB, give highly inaccurate results that are not sufficient for precise evaluation and circuit optimization [53].

Considering the required computational resources and complex methods for theoretical model creation for correct RF-DC conversion efficiency and WPT performance estimation, the current work is based on experimental studies.

1.3. Conclusions on theoretical analysis of WPT technology

The current chapter summarises and analyses different WPT techniques in near-field and far-field regions. Electromagnetic radiative radiation has been selected as more suitable for autonomous powering of sensor nodes .

The theoretical analyses of studies on RF WPT have shown the following:

- The most popular and promising topology of the rectifier in terms of RF-DC conversion efficiency is the voltage doubler.
- The input power level in the case of autonomous powering of sensor nodes via RF WPT is sufficiently low; therefore, the circuit of the power harvester should be optimised to low input power levels – around 0 dBm and lower.
- The lower frequency ranges used for WPT could provide large distance or higher average input power levels for autonomous powering of sensor nodes.
- The impact of the properties of the power-carrying signals on WPT performance is not sufficiently studied yet.
- The research approaches based only on a theoretical analysis could not give sufficiently accurate and calculation resource-saving results.

2. RF-DC circuit prototyping

This section is dedicated to the design of rectifiers – voltage doublers and to the Powercast P2110B module accessible in the market. Modelling of the component impact on the power conversion performance, prototyping of the RF-DC converters, and comparing of the theoretical and experimental rectifier’s performance have been performed. The parameters of rectifiers are optimised to the ISM 863-870 MHz frequency range, input power level around and below 0 dBm and input impedance of 50 Ω .

2.1. Model development and simulation

One of the selection criteria for the rectifier’s components was the price, the other was the availability of the components and materials. Therefore, from the chosen criteria, the most appropriate PCB material is FR-4 (flame retardant 4), whose performance is acceptable in the

sub-GHz frequency range. The impact of PCB material on RF-DC conversion efficiency is summarised in Table 1.1. In this frequency range, the dielectric loss of the FR-4 material is worse than the ceramic substrate Rogers RO4350B; however, for the current application, it is acceptable [54], [55].

There is a wide range of diodes with similar parameters that are suitable for the RF-DC power conversion in the sub-GHz frequency range, such as Infineon BAT 63-02V [56], Skyworks SMS7630 [57], and HSMS-2850/285C [58]. Theoretical calculations in [3] show that to increase the RF-DC power conversion efficiency, it is necessary to select the diode with low diode junction capacitance C_{j0} and low series resistance R_s .

Therefore, taking into account the previous considerations, the simulation model contains 2-layer PCB material and the specified dielectric material dielectric constant of FR4 is set to 4.2. The distance between the copper plates is set to 1.6mm. The size and length of PCB traces are kept short. The length of the traces is set according to the necessary minimum space for the component placement and soldering. The PCB traces in the simulation are substituted with the transmission line segments and the corresponding model, and the diode model is taken from the built-in library. The rectifier component values were simulated in a wide range to see the trend of impact of the components on rectification efficiency and, therefore, find the optimal values for achieving the highest power conversion efficiency. The component value range for the simulation was selected in a wide range to find values that allow maximum rectifier performance.

The schematic of the RF-DC converter with the matching network is shown in Fig. 2.1 and consists of the matching network, the clamper, rectifying diode and the low pass filter and load resistance. The copper top layer PCB traces are shown in Fig. 2.2.

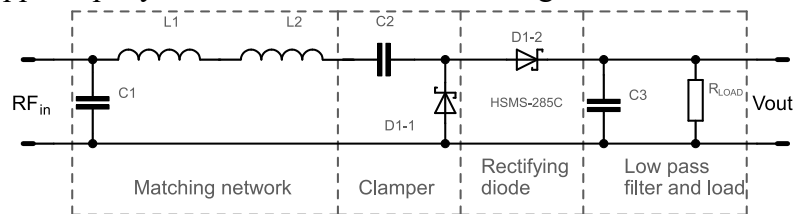


Fig. 2.1. Schematic of the voltage doubler with the matching network.

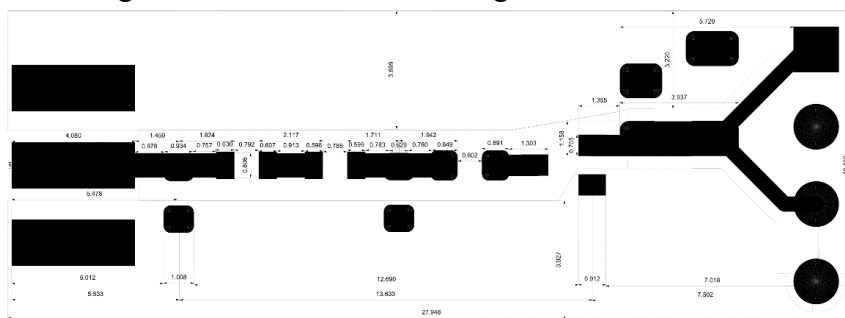


Fig. 2.2. PCB layout of the voltage doubler with the matching network.

However, the Powercast module P2110B simulation was not performed due to the un-accessible schematic; therefore, the simulation model cannot be created.

2.2. Modelling

The modelling of the RF-DC converter was performed in the ADS software using the RF simulation package, employing the harmonic balance method (HBM) solver. Additional components were added for the matching network to allow more tuning capabilities after manufacturing the prototype.

Table 2.1

RF-DC Voltage Doubler with the Matching Network Simulation Parameters

Input power level, dBm	-20 to +2
Frequency range, MHz	863–870
C_2 , pF	1–40
C_3 , μ F	0.01–10
L ($L_1 + L_2$) matching at specified C (C_1) matching values (0.1 to 10) pF; nH	10, 20, 30, 40, 50, 60
C (C_1) matching at specified L ($L_1 + L_2$) matching values (1 to 120) nH; pF	0.5, 1, 2, 3, 4, 5
R Load resistor, $k\Omega$	0.01–40

In the simulation, the rectifier's component values were swept in a wide range to find the combination that would provide the optimal performance, the range of the values shown in Table 2.1.

After multiple iterations of component value sweep, the following component values were selected as in simulation: the matching inductor value sweep range was from 10 nH to 60nH with the step of 10 nH value. The matching capacitor value sweep was performed from 0.1 pF to 10 pF values.

The rectified voltage and power conversion efficiency simulation with parametric matching capacitance values sweep at the specified 6 inductor matching values are shown in Fig. 2.3. The matching network inductance simulation indicates that inductor values, for example 10 or 20, or 30 nH, are not the optimal values. The peak rectified voltage cannot be achieved varying the matching capacitance value, additionally, with these inductor values, the increase of the matching capacitance will decrease the rectified voltage.

In these sweeping component value simulation series, the highest rectified voltage, shown in Fig. 2.3, is achieved with the matching network inductor value of 40 nH and the matching capacitor value of approximately 1.8 pF value. There is only one voltage peak in the graph. For the inductor values that are much higher than 40 nH, the rectified voltage peaks decrease significantly and produce multiple local maximum peaks. Therefore, the optimal value for the matching inductor is 40 nH. The efficiency of the rectifier is calculated by dividing the power across the resistor by the signal input power level at the rectifier's input. The highest efficiency in this simulation with the optimally selected component values yield 82.5 %.

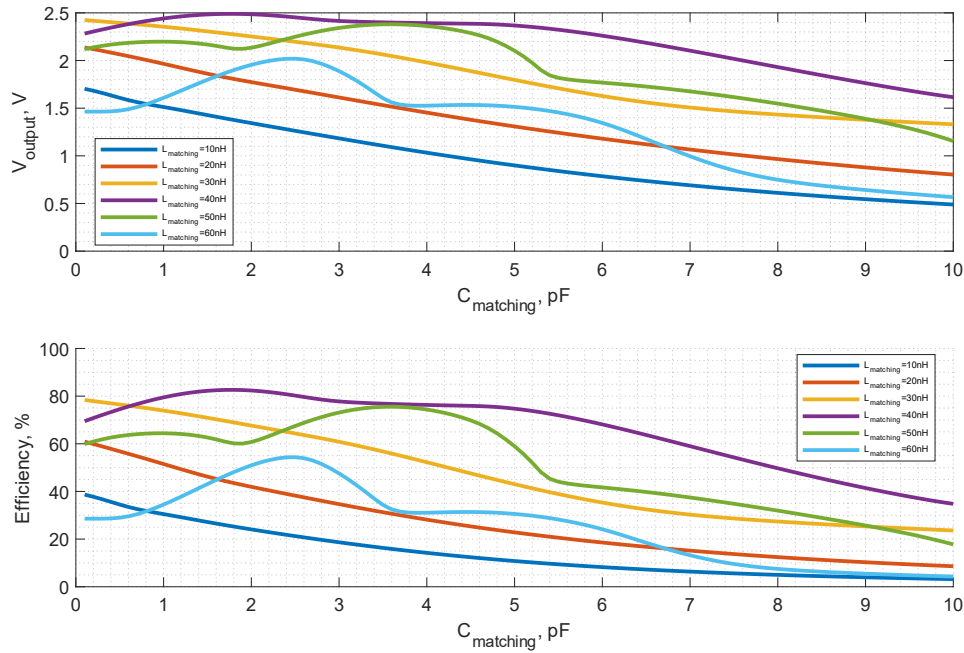


Fig. 2.3. Matched RF-DC voltage doubler output voltage and conversion efficiency depending on the matching capacitor value, $C_2 = 8.2 \text{ pF}$; $C_3 = 1 \text{ }\mu\text{F}$; $R_{\text{load}} = 7.5 \text{ k}\Omega$; frequency is 865.5 MHz; input power is 0 dBm.

The following graphs include the results from the sweep simulation, where the matching network capacitance is constant, and the matching network inductance is swept in the defined range. In this simulation, the matching network inductance is swept from 1 nH to 120 nH at constant matching network capacitance values of 0.5, 1, 2, 3, 4, 5 pF.

The rectified voltage dependence from the exact value of the matching network inductance is more dominant, and the matching network capacitance has a much less impact on the rectified voltage level. The near-maximum rectified voltage can be achieved with multiple combinations of matching network capacitance and inductance values with all tested matching network capacitance values. However, the highest rectified voltage is obtained using matching networks capacitance of 3 pF and inductance of 41 nH when the voltage level reaches 2.5 V and the efficiency reaches 83 %; therefore, these values are used in the following simulations.

After obtaining the matching network's optimal parameters, the impact of the remaining rectifier's circuit component values was analysed. Therefore, the impact of capacitor C_2 was evaluated, where the value was varied from 1pF to 40 pF. The simulation shows that the input capacitor value has a minor impact on the rectified DC voltage level in the modelled capacitance range. The same is also true for the power conversion efficiency.

As the load resistance increases, the rectified output voltage also increases, starting from 0 V with very low impedance to 3.6 V at 40 k Ω load resistance. However, the most efficient power conversion is achieved with the 8.5 k Ω load resistance.

2.3. Measurements of rectifier's input impedance

The prototype of the RF-DC converter circuit was fabricated using milling machine LPKF Proto Mat S103. The circuit components were mounted and soldered on the top layer of PCB made of FR-4 with a dielectric constant of 4.3 (manufacturer-specified). The thickness of the substrate was 1.6 mm.

As the RF-DC rectifiers will use an antenna with the 50Ω impedance and be used in measurements with a 50Ω input impedance, the RF-DC converters must also have a 50Ω input impedance to achieve the highest power conversion efficiency.

After initial modelling and prototyping of the RF-DC converter with optimal component values for the rectifier, the prototype performance did not match the results in the simulation.

Therefore, additional matching network tuning was required to achieve better power conversion efficiency.

The evaluation of the prototype input impedance to the required 50Ω was performed with the vector network analyser (VNA) device, and the evaluating parameter was the scattering parameter S11, which is the input impedance parameter and shows how much of the signal power will be reflected back to the antenna or measuring device.

During the tuning, the most optimal matching parameters for achieving the highest efficiency for the prototyped rectifier with matching network were 36 nH inductance and 3 pF capacitance, which differed from the simulated best matching network parameters. The selected circuit parameters are shown in Fig. 2.4. The final component values are as follows: $C_1 = 3 \text{ pF}$; $C_2 = 8.2 \text{ pF}$; $C_3 = 1 \text{ }\mu\text{F}$; $R_1 = 7.5 \text{ k}\Omega$; $L_1 = L_2 = 18 \text{ nF}$.

The circuit was driven using a coaxial cable with the characteristic impedance of 50Ω . The 50Ω impedance value was chosen to match the readily accessible antenna's impedance and the measurement equipment's input impedance. For the prototype, Schottky diode HSMS-285C was selected for D1 and D2.

Another RF-DC rectifier was prototyped without matching network to investigate the matching network's impact on power conversion efficiency. The schematic is shown in Fig. 2.5.

The commercially available off the shelf RF-DC converter module Powercast module P2110B was also used for comparison.

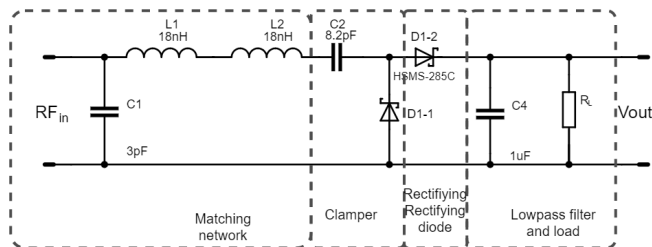


Fig. 2.4. Matched RF-DC voltage doubler schematic with matching network with the component nominals.

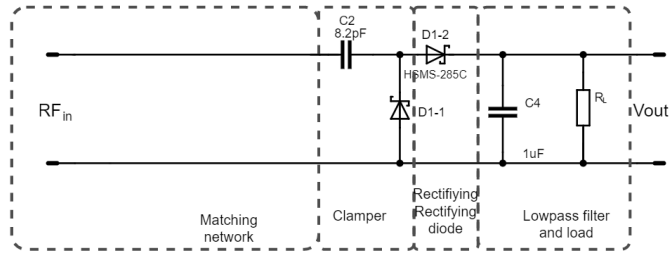


Fig. 2.5. Matched RF-DC voltage doubler schematic without matching network with the component nominals.

Generally, it is considered proper matching if the $|S_{11}|$ scattering parameter is below -10 dB or lower. The Smith chart S_{11} input impedance and the $|S_{11}|$ parameter module are given in Fig 2.6 for the voltage doubler rectifier with matching network, in Fig 2.7 for the voltage doubler rectifier without matching network, and in Fig. 2.8 for the Powercast P2110B module. The results of the input impedance of the voltage doubler rectifier with matching network at different input power levels show a proper matching in the frequency range from 863–870 MHz. The $|S_{11}|$ measurement result for the voltage doubler rectifier without matching network shows poor matching, $|S_{11}|$ does not exceed -0.78 dB at all of the tested signal input power levels. The same input impedance measurements were also performed with the Powercast P2110B module, where the measured $|S_{11}|$ parameter showed good matching.

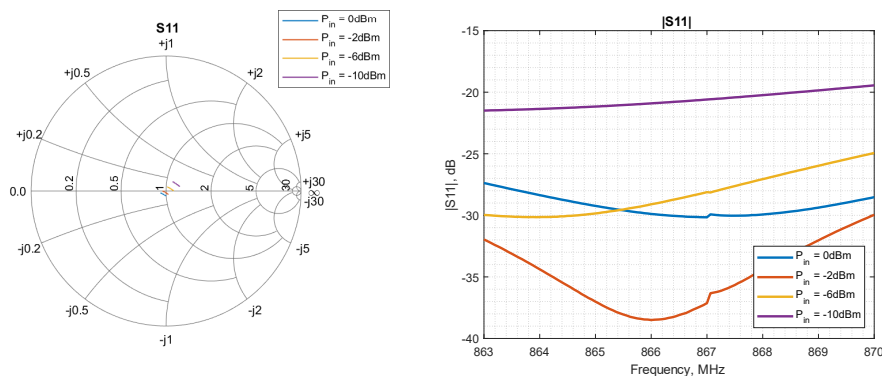


Fig. 2.6. The voltage doubler rectifiers with matching network S_{11} Smith chart and $|S_{11}|$ frequency response at different power levels.

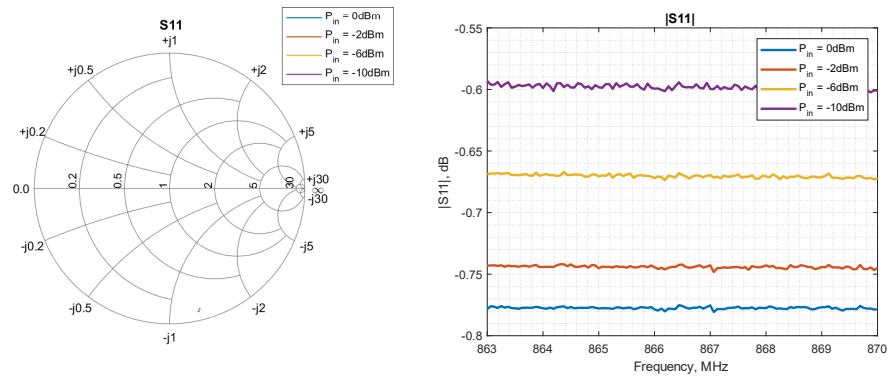


Fig. 2.7. The voltage doubler rectifiers without matching network S11 Smith and $|S_{11}|$ frequency response at different power levels.

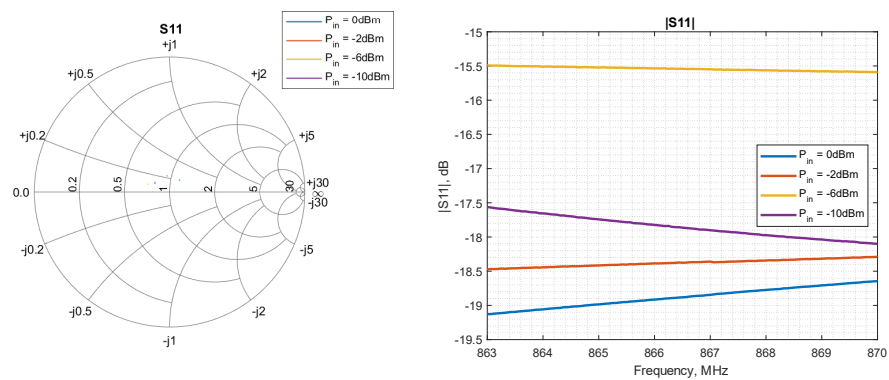


Fig. 2.8. The Powercast P2110B modules S11 Smith and $|S_{11}|$ frequency response at different power levels.

2.4. Conclusions on RF-DC circuit prototyping

In this chapter, simulations and prototyping for ISM 863–870 MHz frequency range, input power level below 0 dBm, and input impedance of 50Ω have been performed. Several prototypes have been fabricated – voltage doubler with and without matching network and Powercast P2110B module. The performance of the rectifiers has also been compared.

The simulation results for the voltage doubler rectifier with matching network show similar performance to the manufactured prototype.

The impedance matching network component values used in the prototype differ from the simulated values; however, no more than by 10 %.

The Smith charts and the corresponding S11 module frequency response graphs show that the voltage doubler with matching network and the Powercast module has an adequate input impedance matched to the 50Ω measurement equipment. Respectively, the signal frequency in the ISM 863-870 MHz band will have little impact on RF-DC conversion performance.

3. Experimental study on RF-DC conversion efficiency

This study is devoted to the investigation of the signal parameters that impact the RF-DC power conversion and are evaluated with multiple RF-DC converters. The parameters that are investigated are as follows:

- signal average input power level;
- signal frequency;
- signal bandwidth;
- number of signal subcarriers.

The investigation includes constant envelope waveforms such as sine wave, FM tonally modulated signals, CHIRP, and variable envelope signal waveforms such as multitone signals with different PAPR levels, see Table 3.1.

Table 3.1

Characteristics of the Employed Signal

Signal envelope	Signal waveform
Constant envelope	sine
	FM tonal modulated signals
	CHIRP (linearly increasing frequency in the selected frequency range)
Variable envelope	multitone signals with high PAPR level (HPAPR)
	multitone signals with low PAPR level (LPAPR)
	multitone signals sub-carriers generated with random seed (RPAPR)

This study was performed with the voltage doubler-based and Powercast RF-DC converters.

The investigation of the different signal parameter impact on the power conversion efficiency is divided into 3 distinctive research directions, which are as follows:

1. Signal waveform impact on the conversion efficiency.
2. Multitone signal subcarrier impact on the conversion efficiency.
3. The matching network impact on conversion efficiency.

The component values of the RF-DC rectifier with matching network and the voltage doubler without matching network are given in Table 3.2, and general schematic of the prototyped rectifier is given in Fig. 3.1. The picture of the RF-DC converter prototyped boards is shown in Fig. 3.2: a) – voltage doubler with matching network; b) – voltage doubler without matching network; and c) – Powercast module P2110B.

Table 3.2

Parameters of Experimental RF-DC Rectifiers

Rectifiers	Components					
	C_1, pF	L_1, nH	L_2, nH	$D1, D2$	$C_3, \mu F$	$R_1, k\Omega$
RF-DC voltage doubler rectifier without matching network	–	–	–	HSMS-285C	$1 \pm 10 \%$	$7.5 \pm 0.1 \%$
RF-DC voltage doubler rectifier with matching network	3 ± 0.1	$18 \pm 5 \%$	$18 \pm 5 \%$	HSMS-285C	$1 \pm 10 \%$	$7.5 \pm 0.1 \%$

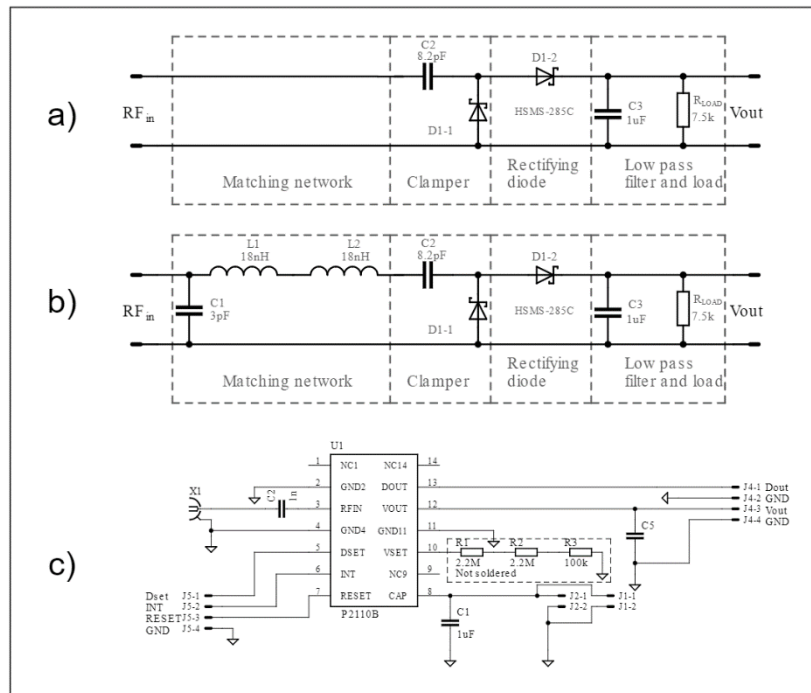


Fig. 3.1. The RF-DC rectifiers schematics: a) RF-DC voltage doubler without matching network; b) RF-DC voltage doubler with matching network; c) Powercast P2110B module.

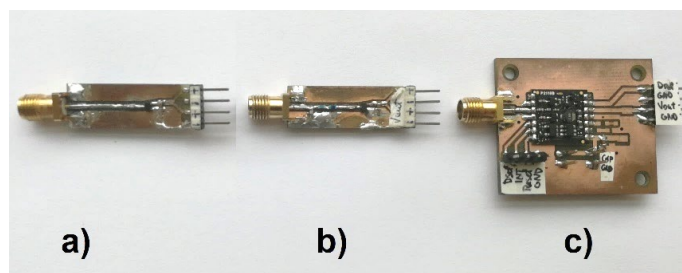


Fig. 3.2. The RF rectifier prototypes: a) RF-DC voltage doubler without matching network, b) RF-DC voltage doubler with matching network, c) Powercast P2110B converter module.

The generation of signals is performed using universal software radio peripheral (USRP) software-defined radio device (SDR) B210 from the Ettus Research company.

The measurement setup of the RF-DC measurements is shown in Fig. 3.3. It consists of two parts: A) – where the average input power level for the signal is calculated; and B) – where the RF-DC measurements are performed, and the DC voltage is measured across the rectifier's load resistance. The devices used in the measurements consist of a host PC with MATLAB/SIMULINK software, the USRP SDR B210, digital oscilloscope Tektronix DPO-72004C and PSMU unit Keysight B2901A. The output power of the RF-DC rectifier is calculated by squaring the rectified DC voltage across the load resistance. The measurement with the Keysight PSMU is automated using MATLAB scripts developed by the author.

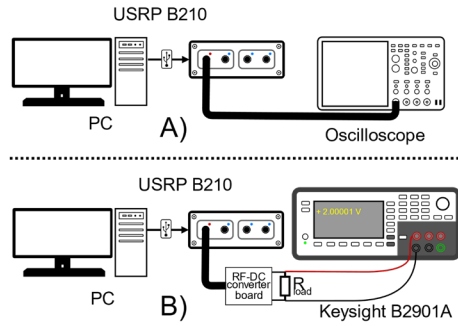


Fig. 3.3. RF-DC Measurement setup.

3.1. Signal waveform impact on the power conversion efficiency

3.1.1. Objective

The objective of this chapter is to study the signal waveform impact on the RF-DC power conversion efficiency. In this study, the research focuses on the signal bandwidth and subcarriers' impact on the RF-DC conversion efficiency.

3.1.2. Tasks

To evaluate the impact of the signal waveform on the RF-DC conversion efficiency, measurement series with the specified types of signals were performed. More detailed information regarding the employed signal parameters is shown in Table 3.3.

Table 3.3

RF Signal Parameters

Signal waveform	Sine	HPAPR	LPAPR	RPAPR	FM	CHIRP
Average power level	-25 dBm to 2 dBm					
Signal bandwidth	-	50 kHz, 500 kHz, 5 MHz			5 MHz	150 kHz
Subcarriers	1	8			Modulation index 4.8, 48	-
PAPR level, dB	3	10-33	6-7.5	7.6-12	3	3

3.1.3. Measurement setup and experiments

The measurements are divided into two parts: 1) the signal average input power level is measured for all the signals employed in this experiment, and 2) the signal is fed to the rectifier and the rectified voltage level is measured for the corresponding input signal power level.

The measurements were performed with the RF-DC voltage doubler with the matching network rectifier. The parameters varied in the experiment are given in Table 3.4.

Table 3.4

RF-DC Rectifier Frequency Characterization Parameters

Input power, dBm	-10, -6, -2, 0, 2
frequency, MHz	863–870
Load resistor, k Ω	1, 10, 100

3.1.4. Experimental results

This section shows the RF-DC voltage doubler with the matching network rectifiers' performance with different signals waveforms, signal bandwidths, input power levels, and 3 different load resistor values.

The power conversion efficiency measurements were performed with 3 different load resistor values employing an RF-DC voltage doubler with the matching network; the results are shown in Fig. 3.4. The highest power conversion efficiency of 62 % is achieved with the load resistance of 10 k Ω .

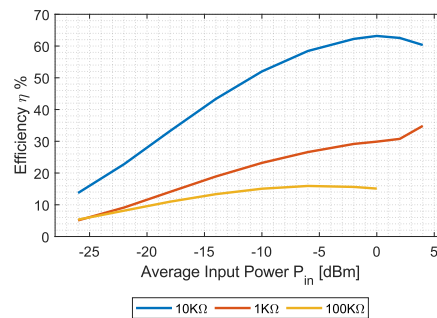


Fig. 3.4. Matched RF-DC voltage doubler with matching network conversion efficiency depending on different load resistances at different input power levels.

The rectifier's performance dependence measurement of the signal frequency was performed with the load resistance of 10 k Ω . The measurement consisted of the sine wave swept in the range from 863 to 870 MHz at 6 different power levels: -10 dBm, -6 dBm, -2 dBm, 0 dBm, and 2 dBm showing uniform performance across the frequency range from 863 to 870 MHz and corresponding efficiency levels 50 %, 57 %, 61 %, 63 %, and 63 %.

Another measurement series were performed [25], where the 3 multitone signals were employed with 3 different bandwidths. In these measurements, HPAPR multitone with high PAPR level, LAPR multitone signal with low PAPR level, and RPAPR multitone signal with three different bandwidths: 50 kHz, 500 kHz, and 5 MHz with 8 subcarriers were employed. The rectified DC voltage a) and the power conversion efficiency b) of power conversion with the multitone signal bandwidths of 5 MHz, 500 kHz and 50 kHz at 3 load resistor values are shown respectively in Figs. 3.5–3.7. For reference, the single-tone sine signal is also added to the figures. From the obtained results it seems that the selected bandwidths do not impact the conversion efficiency. The highest efficiency is obtained in the 10 k Ω load case, while the highest converted voltage in 100 k Ω case. The lower conversion performance is obtained for HPAPR signals with 1 k Ω and 10 k Ω load, correspondingly.

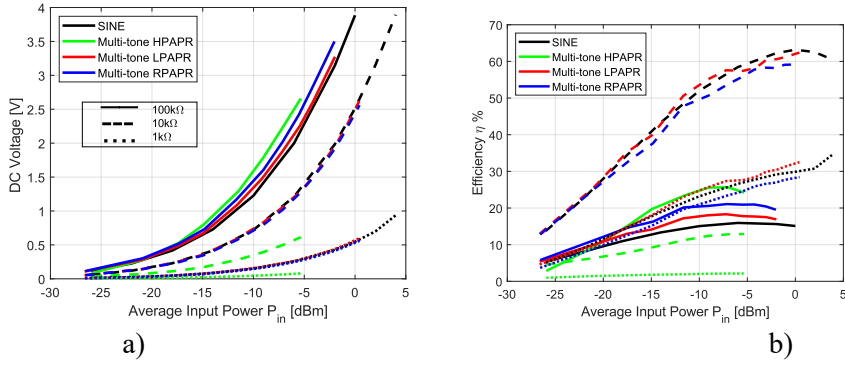


Fig. 3.5. Matched RF-DC voltage doubler output voltage and conversion efficiency depending on the waveform and input power level with 5 MHz bandwidth [25].

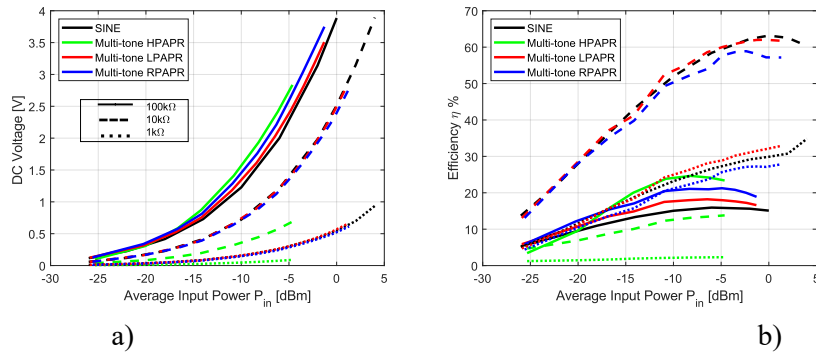


Fig. 3.6. Matched RF-DC voltage doubler: a) output voltage; and b) conversion efficiency depending on the waveform with 500 kHz bandwidth [25].

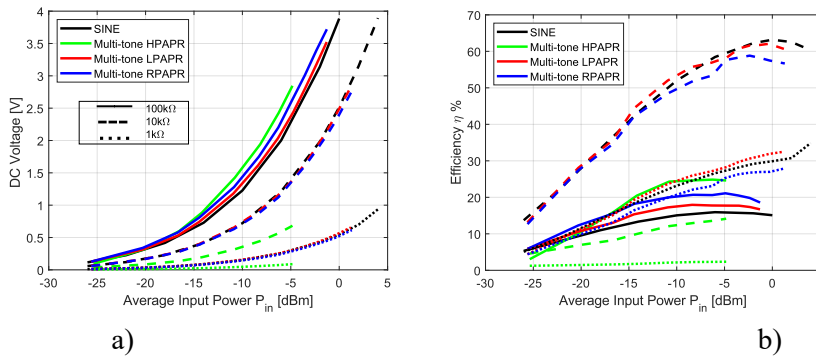


Fig. 3.7. Matched RF-DC voltage doubler: a) output voltage; and b) conversion efficiency depending on the waveform and input power level with 50 kHz bandwidth [25].

The power conversion of the constant envelope signal produced similar power conversion efficiency as the sine waveform. The results are shown in Figs. 3.8 and 3.9.

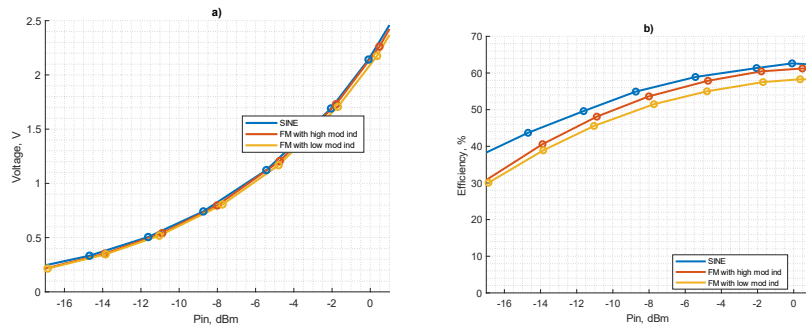


Fig. 3.8. Rectified a) DC voltage and b) conversion efficiency with FM tonal modulated signal with high modulation index and low modulation index employing RF-DC voltage doubler converter with matching network.

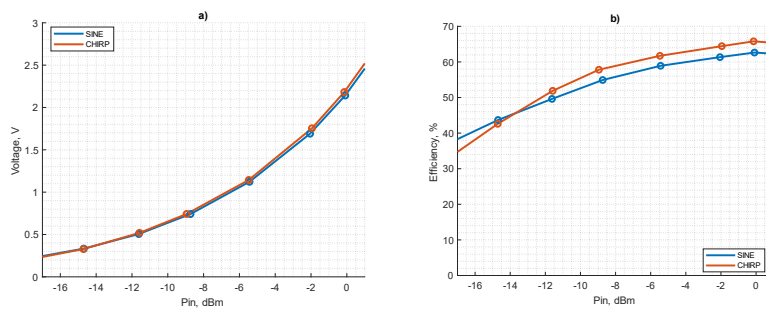


Fig. 3.9. Rectified a) DC voltage and b) conversion efficiency with CHIRP signal employing RF-DC voltage doubler converter with matching network at 7.5 k Ω .

3.1.5. Summary of the signal waveform impact on power conversion efficiency

The reviewed signal waveforms in the RF-DC conversion with the voltage doubler with matching network show that the constant envelope signals and the LPAPR and RPAPR multitone waveforms provide similar power conversion efficiency as the sine with the voltage doubler rectifier with matching network. The multitone signal bandwidth impact on the rectifier is minimal and provides similar power conversion efficiency with the 50 kHz, 500 kHz, or 5 MHz bandwidth.

3.2. Impact of the number of multitone signal subcarriers on power conversion efficiency

3.2.1. Objective

This section is dedicated to the study of the subcarrier impact on the conversion efficiency with the RF-DC voltage doubler rectifier, matching network, and the Powercast P2110B module. This section reviews 3 different multitone signal waveforms with a number of subcarriers ranging from 4 to 256. The RF-DC conversion load resistance impact is evaluated in more detail with different signal waveforms and subcarriers.

3.2.2. Tasks

To investigate the impact of the number of subcarriers on the power conversion efficiency, the RF-DC measurement series are performed with three types of signal waveforms: HPAPR, LPPAR, and RPAPR, with the number of subcarriers in the range from 4 to 256.

3.2.3. Measurement setup

The RF-DC power conversion measurement series were performed with 3 multitone signals. The measurement setup and the signal generation algorithms are already described at the beginning of Chapter 3. The summary of signal parameters is given in Table 3.5.

Table 3.5

RF Signal Parameters

Signal waveform	Sine	HPAPR	LPAPR	RPAPR
Average power level	-17 dBm to 0 dBm			
Signal bandwidth	-	5 MHz		
Subcarriers	1	4-256		
PAPR level, dB	3	10-33	6-7.5	7.6-12

3.2.4. Experimental results

In these experiments, the multitone subcarrier impact on the RF-DC conversion efficiency was evaluated with 3 different signal waveforms: HPAPR, LPAPR, and RPAPR multitone. The RF-DC voltage doubler rectifiers' performance with matching network is given in Figs. 3.10-3.12, the rectified DC voltage across the load resistance value is given in graph a), and the power conversion efficiency is given in graph b).

The prototyped RF-DC rectifier's performance with matching network employing the HPAPR multitone signal with different subcarriers is given in Fig. 3.10. The power conversion is not only dependent on the signal waveform but also the number of subcarriers. The increase of the number of subcarriers decreases the converted output voltage across the resistance load, and the power conversion efficiency overall is lower than using the sine signal. While the conversion performance in the case of LPAPR and RPAPR signals is quite similar to sine signal as is presented in Figs. 3.11 and 3.12.

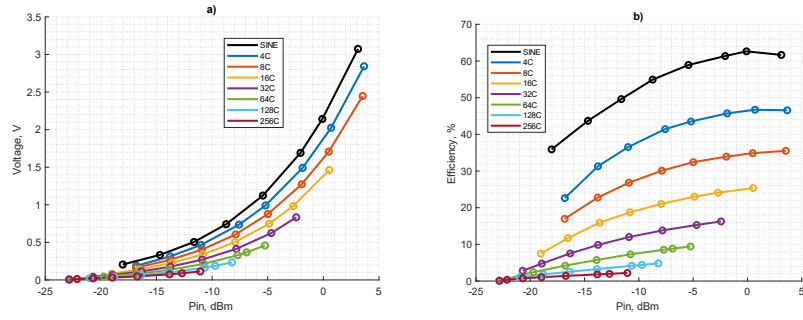


Fig. 3.10. Rectified a) DC voltage and b) conversion efficiency with HPAPR multitone signal with subcarrier count from 4 to 256 employing the RF-DC voltage doubler converter with matching network.

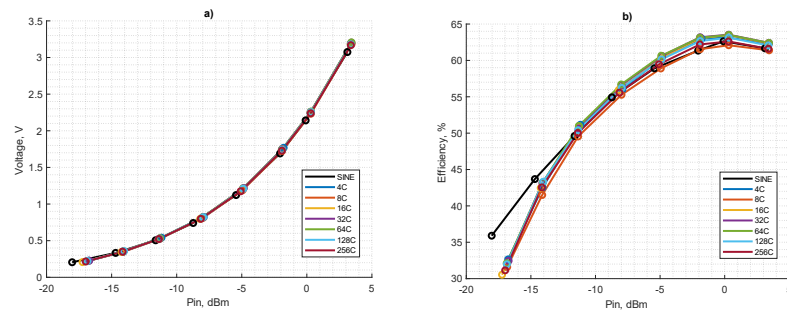


Fig. 3.11. Rectified a) DC voltage and b) conversion efficiency with LPAPR multitone signal with subcarrier count from 4 to 256 employing the RF-DC voltage doubler converter with matching network.

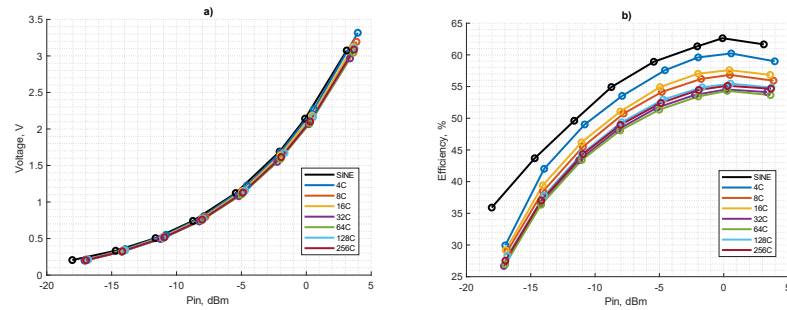


Fig. 3.12. Rectified a) DC voltage and b) conversion efficiency with RPAPR multitone signal (random carrier amplitude and phase) with subcarrier count from 4 to 256 employing the RF-DC voltage doubler converter with matching network.

The performance of the commercially available RF-DC converter Powercast P2110B is shown in Fig. 3.13, where the rectified voltage a) and the power conversion efficiency b) depending on the HPAPR multitone input signal average power level and different subcarrier value is shown. The Powercast converter overall performance with HPAPR multitone signal waveform shows a similar trend as with the RF-DC voltage doubler with matching network: increasing the number of subcarriers leads to the decrease of the overall power conversion efficiency at the same input power level, however, the efficiency decrease with the Powercast module is less steep compared to the voltage doubler with matching network.

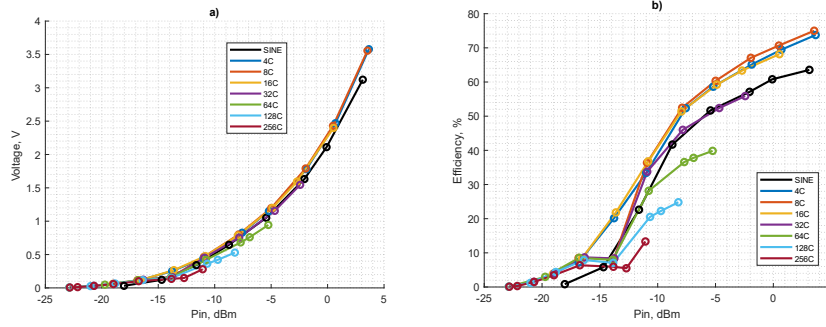


Fig. 3.13. Rectified a) DC voltage and b) conversion efficiency with high PAPR multitone signal with subcarrier count from 4 to 256 employing the RF-DC converter module Powercast P2110B.

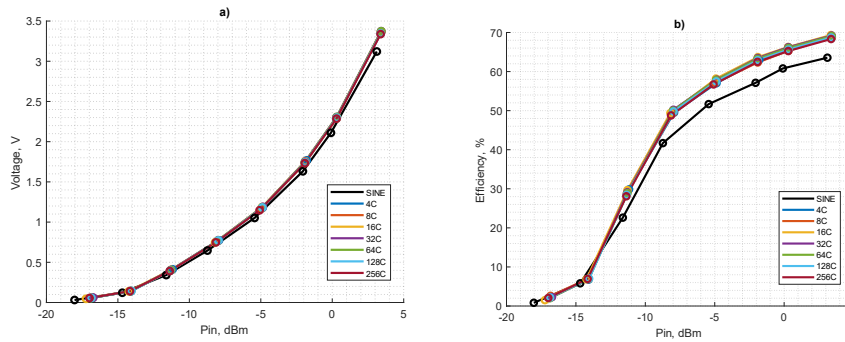


Fig. 3.14. Rectified a) DC voltage and b) conversion efficiency with low PAPR multitone signal with subcarrier count from 4 to 256 employing the RF-DC converter module Powercast P2110B.

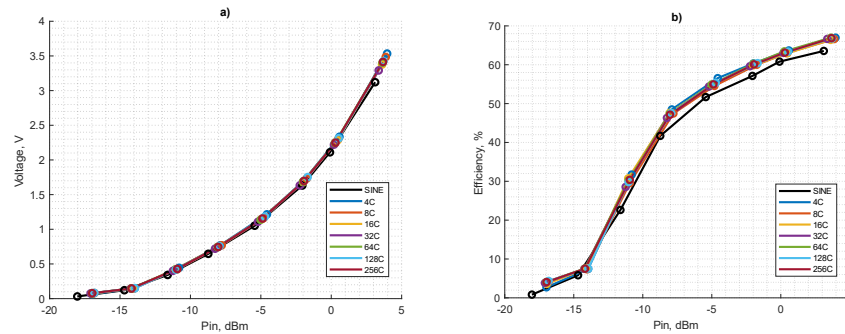


Fig. 3.15. Rectified a) DC voltage and b) conversion efficiency with RPAPR multitone signal (random carrier amplitude and phase) with subcarrier count from 4 to 256 employing the RF-DC converter module Powercast P2110B.

RF-DC power conversion of the Powercast module using the LPAPR and RPAPR multitone signals shows a similar trend as the RF-DC voltage doubler rectifier with matching network. The number of subcarriers of the LPAPR and RPAPR multitone signal has minimal impact on the power conversion efficiency with the Powercast module. The Powercast converter delivers the same power conversion efficiency irrespective of the number of tested subcarriers (see Figs. 3.14 and 3.15).

The previous experimental data shows that the power conversion efficiency is dependent on the signal waveform, input power level, and resistance load with the sine wave: it is

hypothesized that the power conversion with different waveform signals will also be dependent on the input power level and load resistance. The RF-DC conversion is also dependent on the frequency. However, the performed frequency measurements show that the voltage doubler with matching network can be considered frequency independent in the specified ISM frequency range from 863 to 870 MHz. Therefore, additional RF-DC power conversion experiments were performed, where the load resistance value varied from 1 kΩ to 200 kΩ. The following measurements with the variable resistor load were performed with a voltage doubler converter. Another measurement series were performed with the RF-DC voltage doubler with matching network using different level multitone signals with a number of subcarriers from 4 to 64.

The LPAPR multitone signal has similar PAPR level as the RPAPR multitone signal. Therefore, only HPAPR and LPAPR multitone signal waveforms were investigated for the power conversion efficiency dependence from the load resistance value, see Figs. 3.16 and 3.17, where the rectified DC voltage is shown in part a) and the power conversion efficiency is shown in part b). The results show that using the HPAPR multitone signal the resistance value, at which the most efficiency is achieved, changes depending on the number of subcarriers. For example, when using the HPAPR multitone signal with 4 subcarriers, the most optimal load resistance value is 23 kΩ, with 8 subcarriers multitone signal – 35 kΩ, and so on. Also, with the increase of subcarriers, the achievable peak efficiency decreases.

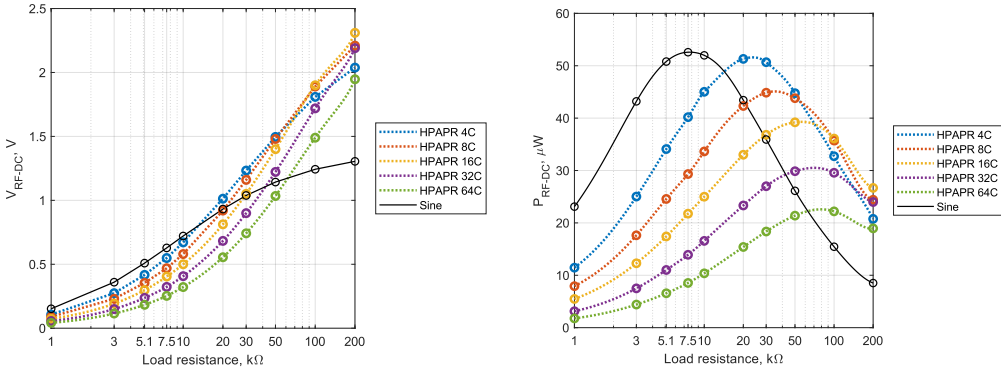


Fig. 3.16. Rectified a) DC voltage and b) conversion efficiency with high PAPR level multitone signal with subcarrier count from 4 to 64 employing the RF-DC voltage doubler converter with matching network with different load resistance value at -10 dBm input power level.

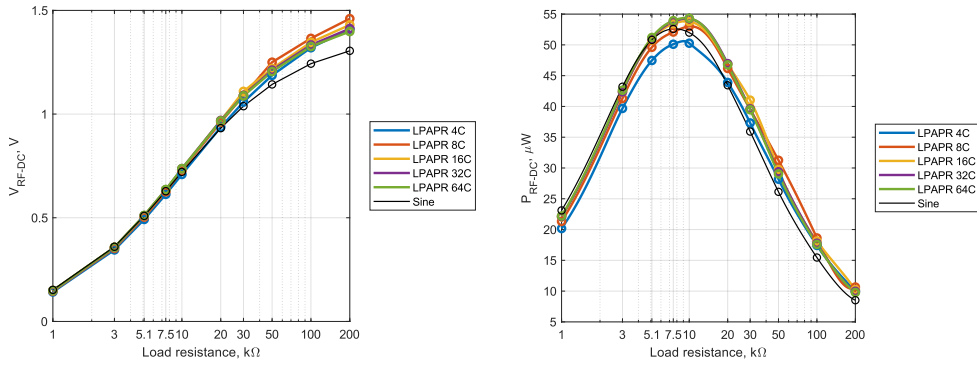


Fig. 3.17. Rectified a) DC voltage and b) conversion efficiency with low PAPR level multitone signal with subcarrier count from 4 to 64 employing the RF-DC voltage doubler converter with matching network with different load resistance value at -10 dBm input power level.

3.2.5. Summary of impact of the number of multitone signal subcarriers on the power conversion efficiency

The FM modulated, CHIRP, LPAPR, and RPAPR multitone signal use in the power conversion with the RF-DC voltage doubler rectifier with matching network give quite the same results as in the case of sine signal employment. The measurements with the voltage doubler with matching network using the HPAPR multitone signals in the ISM sub-GHz frequency range from 863 to 870 MHz show that the load resistance value must be adjusted appropriately, depending on the number of subcarriers to reach the peak power conversion.

3.3. Matching network impact on the RF-DC conversion efficiency

3.3.1. Objective

This experiment series is dedicated to the study of the matching network impact on the RF-DC power conversion efficiency. This section studies the voltage doubler with and without matching network with the HPAPR multitone signal.

3.3.2. Tasks

This research aims to evaluate the impact of matching network on the power conversion efficiency; therefore, the same rectifier with and without matching network was prototyped.

3.3.3. Measurement setup and experiments

The measurements are divided into two parts: 1) where the signal average input power level is measured for all the signals that are employed in this experiment; and 2) where the signal is fed to the rectifier, and the rectified voltage level is measured for the corresponding input power level, the signal parameters are shown in Table 3.6.

Table 3.6

RF Signal Parameters

Signal waveform	Sine	HPAPR	LPAPR	RPAPR	FM	CHIRP
Average power level	-17 dBm to 0 dBm					
Signal bandwidth	-	5 MHz			5 MHz	150 kHz
Subcarriers	1	4-256			Modulation index 4.8, 48	-
PAPR level, dB	3	10-33	6-7.5	7.6-12	3	3

3.3.4. Experimental results

The power conversion measurements have been performed for the RF-DC rectifier with matching network and without matching network with the voltage doubler topology. The power conversion measurements with different signal waveforms have been produced, including constant envelope and varying envelope signals.

The measurements were performed with the multitone signal with a high PAPR level using the rectifier without matching network. Figure 3.18 shows the performance of RF-DC voltage doublers without matching network with high PAPR level multitone signals: a) rectified DC voltage and b) power conversion efficiency. The rectified DC voltage level is dependent on the number of subcarriers, as shown in Fig. 3.19.

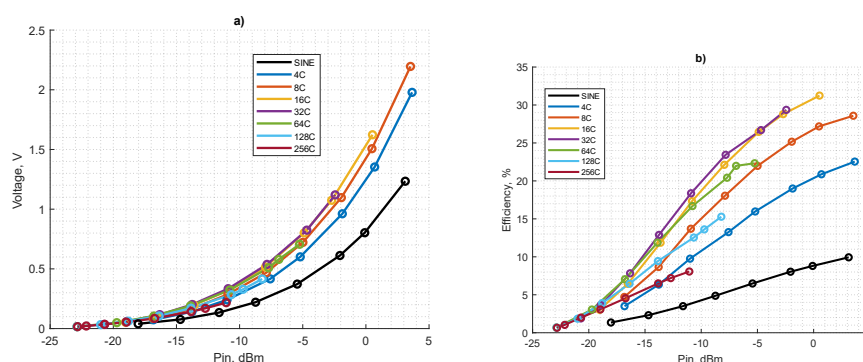


Fig. 3.18. Rectified a) DC voltage and b) conversion efficiency with high PAPR multitone signal with subcarrier count from 4 to 256 employing the RF-DC voltage doubler converter without matching network.

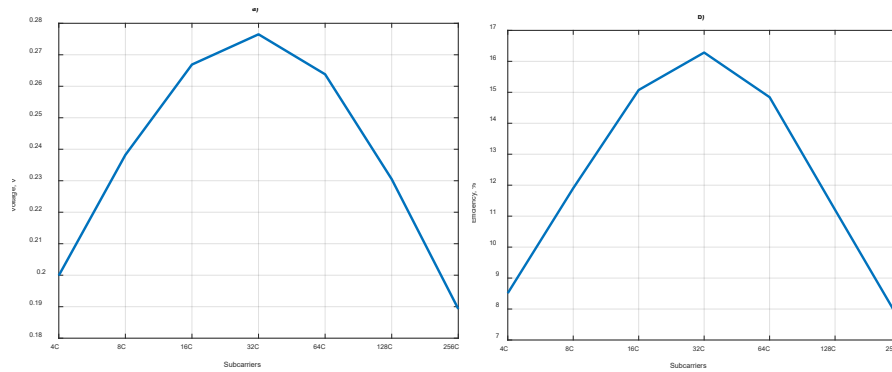


Fig. 3.19. Rectified a) DC voltage and b) conversion efficiency with high PAPR multitone signal input signal at -12 dBm power level with subcarrier count from 4 to 256 employing the RF-DC voltage doubler converter without matching network.

The converter's performance with the LPAPR and RPAPR multitone signals as well as FM tonally modulated and CHIRP signals is relatively low and similar to the performance observed with the sine waveform.

3.3.5. Summary of impact of matching network on the RF-DC conversion efficiency

The impact of matching network on the voltage doubler topology with different signal waveforms has been evaluated. The power conversion employing LPAPR multitone signals with the rectifier without matching network has a similar performance as the sine waveform and the RPAPR multitone signals. In comparison, the impact of the number of multitone subcarriers is limited with the LPAPR multitone and the RPAPR multitone, where efficiency fluctuates correspondingly less than 2 % and 4 % for the tones in the range from 4 to 256. The situation is different with the high PAPR level multitone signals. The power conversion trend of the rectifier with a matching network shows that the increase in subcarrier value will lead to a decrease in the power conversion efficiency. For the RF-DC converter without matching network, the situation is similar. However, there is a corresponding subcarrier value, where the increase of the subcarrier will yield a higher efficiency level than the converter with matching network. The use of the CHIRP signal in power conversion also shows similar power conversion efficiency to the sine waveform, as this signal has the same PAPR level as the sine waveform.

3.4. Conclusions on experimental study on RF-DC conversion efficiency

In the current chapter, the impact of properties of the RF power-carrying signals on RF-DC conversion efficiency for the prototyped RF-DC rectifiers – voltage doubler with and without matching network is evaluated. The experimental study is performed in ISM 863–870 MHz frequency range. The analysed signals have a constant or varying envelope, different levels of average input power, different bandwidths, number of multicarriers, and PAPR level.

During the study, the following main conclusions have been made:

- The constant envelope signals (sine, FM modulated, CHIRP) and the LPAPR and RPAPR multitone waveforms provide the same power conversion efficiency in the case of the voltage doubler rectifier with a matching network.
- The impact of the multitone signal bandwidth on the rectifier performance is minimal for all observed cases (50 KHz, 500 KHz, or 5 MHz).
- The adjustment of the load resistance in correspondence to the number of HPAPR subcarriers increases the RF-DC conversion efficiency for the voltage doubler with matching network.
- The number of subcarriers in the employment of LPAPR and RPAPR multitone power-carrying signals and the voltage doubler without matching network does not sufficiently impact the RF-DC conversion efficiency.
- The increase in the number of HPAPR subcarriers leads to a decrease in the power conversion efficiency in the case of a voltage doubler with matching network.

4. Experimental study on WPT performance

The development of the wireless channel models presents trade-offs between the precision of the model – depicted by the number of physical effects and material properties considered - and the computational time and resources. While the most precise model is desirable, the computational time and power are strictly limiting factors, meaning that reasonably simplified models can have broader applications. However, the results in different environments may present discrepancies that cannot be accounted for with the simulations. The experimental study of the WPT performance aids in developing the theoretical model by narrowing the set of physical properties of the channel down to the most significant ones.

For this reason, experimental studies of the WPT performance in the laboratory were performed. The experimental studies focused on determining the essential transmission parameters by their impacts on the amount of the harvested energy using RF-DC converters. In this investigation, the parameters of interest that influence the WPT are:

- distance between the transmitting and receiving antennas;
- impact of the antenna type on the harvesting level indoors;
- signal frequency impact;
- signal waveform impact.

4.1. Measurement setup

This section describes the measurement setup used to perform the experimental studies on the parameters of the WPT. The measurements were performed using the setup demonstrated in Fig. 4.1. The signal is generated in real-time using MATLAB/SIMULINK software and transferred to software-defined radio (SDR) USRP B210. The signals generated by SDR were also amplified using an external amplifier based on the MMG3006NT1 and MW7IC008N integrated circuits. In the receiver, the antenna's output is connected to the RF-DC converter,

and the output power of the RF-DC converter is measured using the Keysight PSMU B2910A device.

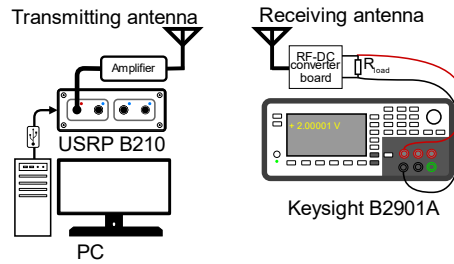


Fig. 4.1. Measurement setup for WPT parametric characterization [59].

4.2. Study of the factors influencing the WPT efficiency

The first study aimed to determine how the power-carrying signal's frequency impacts the received power level. The measurements were performed for several power-carrying signal frequencies and distances between the two antennas. The signal waveform was a sine wave with a 22.3 dBm power level. This experiment swept the power-carrying signal's frequency from 863 MHz to 870 MHz (ISM band), with antenna distances varied from 0.6 to 3 m (1.73 to 8.6 wavelengths), measuring the average output power of the receiving antenna on the 50 Ω load. The antennas were placed at 1m height. Two different pairs of antennas were employed for the measurements: LP0410 directional antennas with a gain of 6 dBi each VERT900 omnidirectional antennas with a gain of 3 dBi each.

The second study aimed to investigate how the different power-carrying signal waveforms influence the harvested voltage from WPT and the impact of the signal characteristics such as the signal's central frequency, bandwidth, and waveform. This experiment was performed for the voltage doubler-based prototype and the commercially available Powercast P2110B module.

The third study investigated how the frequency-modulated (FM) power-carrying signal with different modulation indexes influences the harvested voltage from WPT. The investigation of such waveform is motivated by the potential applications for simultaneous wireless information and power transfer (SWIPT).

4.2.1. Signal frequency impact on the WPT efficiency

This subsection investigates the WPT measurements and the rectified voltage level depending on the signal waveform, the distance between the transmitting and receiving antennas and different antenna types. The first study results are presented in Fig. 4.2. The directional antenna LP0410 is given in Fig. 4.2 a), along with the omnidirectional antenna VERT900 in Fig. 4.2 b). The curves in these figures display the output power of the receiver's antenna at the said distances between the antennas expressed with wavelengths for every power-carrying signal's frequency.

The theoretical power level that could be acquired in the free space with the selected antennas is shown for the 865.5 MHz frequency for reference. This theoretical estimation is based on the Friis transmission formula shown in Equation (4.1):

$$P_r = P_t + D_t + D_r + 20 \cdot \log_{10} \left(\frac{\lambda}{4\pi d} \right) \quad (4.1)$$

where P_r is the power of the receiving antenna; P_t is the power of the transmitting antenna; D_t and D_r are the directivities of the corresponding antennas; λ is the wavelength; and d is the distance between the antennas.

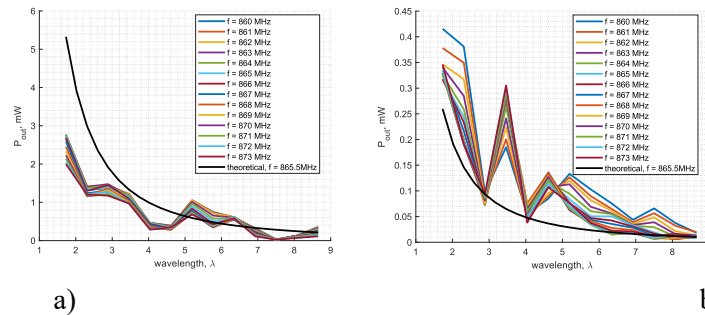


Fig. 4.2. WPT received power level depending on the central frequency using a) directional antennas LP0410 and b) omnidirectional antennas VERT900.

The results of this study indicate that the model of the WPT system is more complex and cannot be precisely estimated just by the Friis transmission equation, as the received power varies with the placement of the antennas.

4.2.2. Signal waveform impact on the WPT efficiency

This subsection is dedicated to studying the signal waveform impact on WPT with different signals, such as multitone signals, tonally modulated FM signals, CHIRP and sine wave as the reference signal.

The results of the second study are presented in Figs. 4.3–4.5. Figure 4.3 shows the output voltage measurements of a) voltage doubler-based RF-DC converter and b) Powercast module for the omnidirectional VERT900 and directional LP0410 antennas using LPAPR power-carrying signal with different numbers of subcarriers. The distances between the antennas are the same as in the previous study. The sine wave results with the same carrier frequency and average power level are compared.

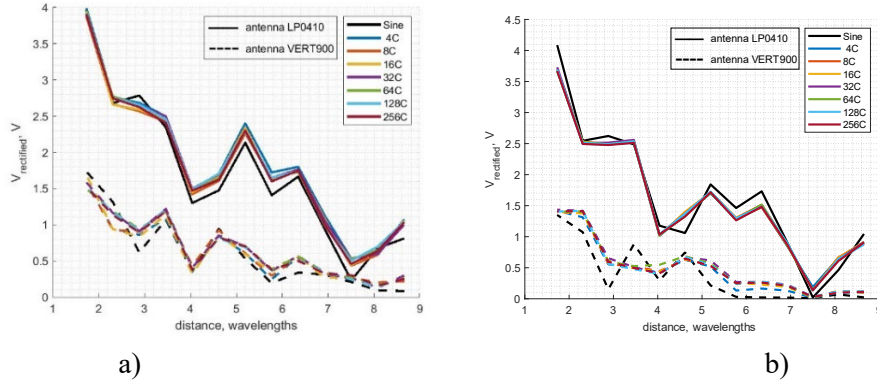


Fig. 4.3. The harvested voltage level of voltage doubler-based RF-DC converter with matching network a) and Powercast P2110B module b) for a different number of LPAPR subcarriers.

Different waveforms show no significant differences in the harvested voltage for distances < 2.2 wavelengths. With distances of more than 4 wavelengths, the LPAPR signals show a greater harvested voltage than the sine wave. For distances less than 4 wavelengths, the number of subcarriers has little effect on the harvested voltage. Using directional antennas with antenna distances of more than 4 wavelengths, the LPAPR signal with 4 subcarriers has greater harvested voltage than the waveforms with different number of subcarriers, although by a small amount. In the case of an omnidirectional antenna, the waveform that gives the highest amount of harvested voltage is different for each antenna placement.

Figure 4.4 shows the measurement results for a) the voltage doubler and b) Powercast using the RPAPR power-carrying signal waveform with different subcarrier numbers. At greater distances (more than 4 wavelengths) the voltage doubler-based RF-DC converter performs better than Powercast P2110B.

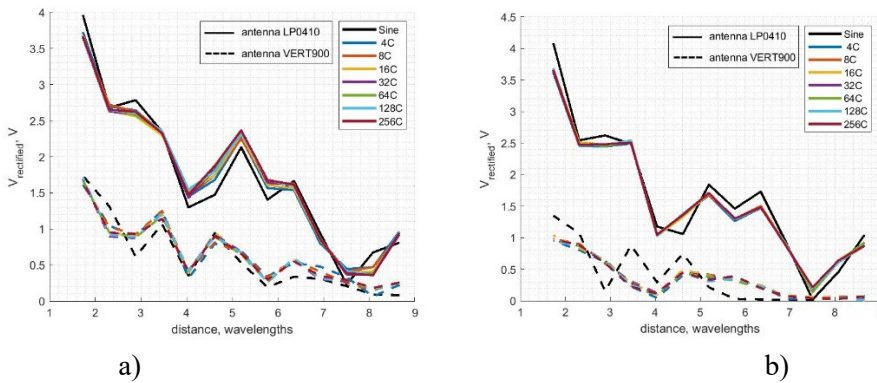


Fig. 4.4. The harvested voltage level of voltage doubler-based RF-DC converter with matching network a) and Powercast P2110B module b) for different number of RPAPR subcarriers.

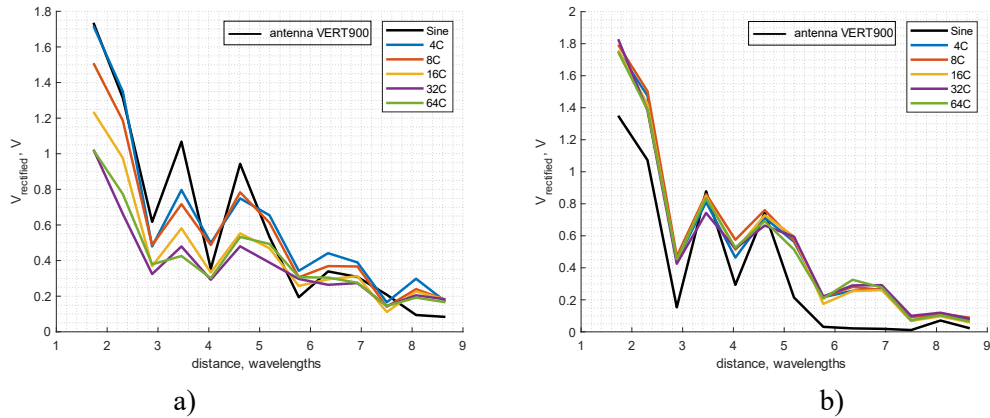


Fig. 4.5. The harvested voltage level of voltage doubler-based RF-DC converter with matching network a) and Powercast P2110B module b) for different number of HPAPR subcarriers.

4.2.3. Impact of constant envelope signal waveform on the WPT efficiency

This subsection is dedicated to the investigation of the converted voltage level in the WPT system depending on the different signal modulation with the same PAPR level and constant envelopes, such as the tonally modulated FM signals, CHIRP, and sine.

The results of the third study are compiled in Figs. 4.6–4.7. Figure 4.6 presents quite similar received average power levels for all observed signals. Figure 4.7 compares the WPT performance of the voltage doubler-based a) and Powercast b) RF-DC converters using directional and omnidirectional antennas. The results in Fig. 4.7 also confirm that the FM modulated signals can be used for WPT with the same efficiency as sinusoidal signals giving additional opportunity to implement simultaneous information and power transmission (SWIPT).

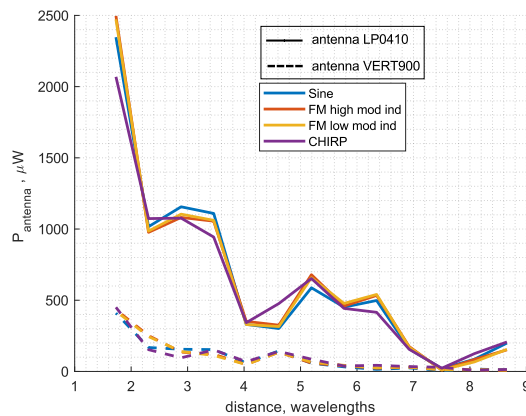


Fig. 4.6. Received average power level at the output of antennas depending on the WPT distance [60].

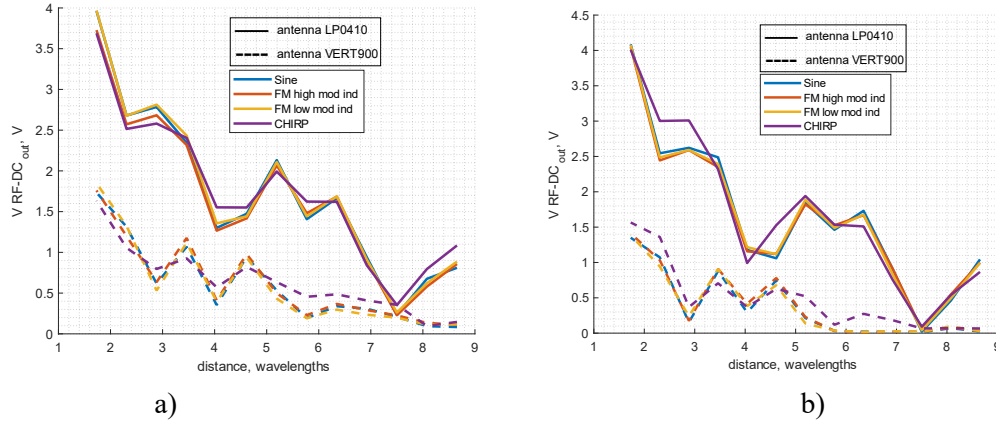


Fig. 4.7. Impact of WPT distance on the RF-DC converted voltage doubler-based RF-DC converter with matching network a) and Powercast P2110B module b) using constant envelope signals [60].

4.3. Conclusions of experimental study on WPT performance

The experimental studies provided in this section aimed to investigate wireless power transfer considering different parameters of power-carrying signals, different types of antennas and the distance between them in the case of a direct line of sight. For the study, the prototyped RF-DC rectifiers – voltage doubler with matching network and Powercast P2110B module have been used in ISM 863–870 MHz frequency range with directional and omnidirectional antennas.

The performed study showed that the following:

- The use of more complex waveforms has particular benefits for WPT – the use of multicarrier signals allows for more efficient energy harvesting. In contrast, the use of FM signals opens possibilities for simultaneous information and power transmission.
- The level of the received average power on the harvester side has a dependence on the signal frequency, which could be explained by the difference in the multipath propagation for observed frequencies in ISM 863–870 MHz range for enclosed space.
- The voltage doubler-based RF-DC converter matches and even exceeds the performance of the commercially available Powercast P2110B RF-DC converter.
- The Friis equation does not provide sufficient approximation to estimate the average received power at the harvester side and evaluate WPT performance for enclosed space.
- The constant envelope signals with the exact power level yield a similar converted voltage level and, therefore, can be combined with SWIPT systems. The simultaneous data and power can be delivered to the needed device (sensor node).

Conclusions

This work was dedicated to the experimental study of the RF signal parameter impact on the RF-DC power conversion efficiency and the wireless power transfer performance. The main subject of research was the employment of the voltage doubler for wireless power transfer in ISM 863–870 MHz frequency range with different types of power-carrying signals.

The following tasks have been performed to reach the set goal:

- Theoretical analysis of the RF-DC rectifier, including the development of a model and the optimization of its parameters was performed.
- Prototypes for different RF-DC converter solutions were designed and fabricated.
- Experimental study on the RF-DC power conversion efficiency of the developed RF-DC converter modules, depending on the RF signal parameters was performed.
- Experimental study on the wireless power transfer performance of the developed RF-DC converter modules depending on the RF signal parameters and antenna type was performed.

The following RF-DC conversion efficiency optimization abilities have been investigated as a result of the research:

- The appropriate adjustment of the voltage doubler converter's load resistance to the number of subcarriers, in case of equal synphase multitone signals with uniformly distributed subcarriers, increase the power conversion efficiency.
- The exclusion of matching network for the voltage doubler, applying equal synphase multitone signals with uniformly distributed subcarriers, increases the RF-DC power conversion efficiency.
- CHIRP signals, tonally modulated FM, and the amplitude modulated signals with PAPR level below 10 dB provide equal power conversion efficiency.

The efficiency analysis of the different WPT signal waveforms has been performed and the results show that the application of the CHIRP, FM tonally modulated, and the amplitude modulated signals with PAPR level below 10 dB in the case of the direct line of sight ensures the same WPT performance as a sine signal.

The obtained knowledge can be used for autonomous sensor node deployment, harvesting circuit topology optimization, as well as for estimation of the effect of a power-carrying signal waveform on the overall WPT system efficiency for an indoor environment use case.

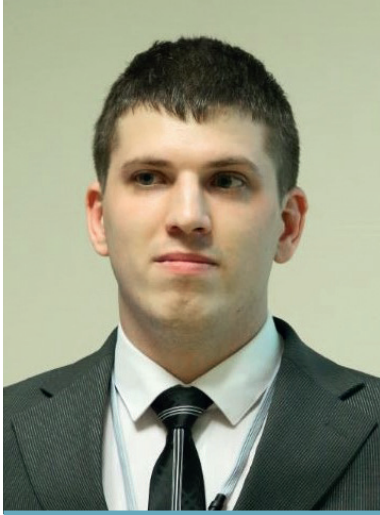
Bibliography

- [1] “Ericsson Mobility Report 2021,” 2021. [Online]. Available: <https://www.ericsson.com/492615/assets/local/reports-papers/mobility-report/documents/emr-quarterly2021-update.pdf>.
- [2] D. Pradeep Kumar Reddy and J. Mohana, *Wireless power transfer: Between Distance and Efficiency*, vol. 8, no. 4, 2016.
- [3] The Institution of Engineering and Technology, *Wireless Power Transfer: Theory, technology, and applications*. Institution of Engineering and Technology, 2018.
- [4] X. Lu, P. Wang, D. Niyato, D. I. Kim, and Z. Han, “Wireless networks with rf energy harvesting: A contemporary survey,” *IEEE Commun. Surv. Tutorials*, vol. 17, no. 2, pp. 757–789, 2015.
- [5] M. A. Houran, X. Yang, and W. Chen, “Magnetically coupled resonance wpt: Review of compensation topologies, resonator structures with misalignment, and emi diagnostics,” *Electron.*, vol. 7, no. 11, 2018.
- [6] J. Eidaks, R. Kusnins, R. Babajans, D. Cirjulina, J. Semenjak, and A. Litvinenko, “Fast and Accurate Approach to RF-DC Conversion Efficiency Estimation for Multi-Tone Signals,” *Sensors*, vol. 22, no. 3, p. 787, Jan. 2022.
- [7] N. Shinohara, K. Nishikawa, T. Seki, and K. Hiraga, “Development of 24 GHz rectennas for fixed wireless access,” *2011 30th URSI Gen. Assem. Sci. Symp. URSIGASS 2011*, pp. 3–6, 2011.
- [8] W. S. High-impedance, “A 5 . 8-GHz Band Highly Efficient 1-W Rectenna,” vol. 69, no. 7, pp. 3558–3566, 2021.
- [9] N. Singh, B. K. Kanaujia, M. T. Beg, Mainuddin, T. Khan, and S. Kumar, “A dual polarized multiband rectenna for RF energy harvesting,” *AEU – Int. J. Electron. Commun.*, vol. 93, no. February, pp. 123–131, 2018.
- [10] Young-Ho Suh and Kai Chang, “A high-efficiency dual-frequency rectenna for 2.45- and 5.8-GHz wireless power transmission,” *IEEE Trans. Microw. Theory Tech.*, vol. 50, no. 7, pp. 1784–1789, Jul. 2002.
- [11] C. Wang, B. Yang, and N. Shinohara, “Study and Design of a 2.45-GHz Rectifier Achieving 91% Efficiency at 5-W Input Power,” *IEEE Microw. Wirel. Components Lett.*, vol. 31, no. 1, pp. 76–79, 2021.
- [12] T. C. Yo, C. M. Lee, C. M. Hsu, and C. H. Luo, “Compact circularly polarized rectenna with unbalanced circular slots,” *IEEE Trans. Antennas Propag.*, vol. 56, no. 3, pp. 882–886, 2008.
- [13] Y. T. Chang, S. Claessens, S. Pollin, and D. Schreurs, “A Wideband Efficient Rectifier Design for SWIPT,” *2019 IEEE Wirel. Power Transf. Conf. WPTC 2019*, pp. 26–29, 2019.
- [14] D. Wang and R. Negra, “Design of a dual-band rectifier for wireless power transmission,” *2013 IEEE Wirel. Power Transf. WPT 2013*, pp. 127–130, 2013.
- [15] M. Ito *et al.*, “High efficient bridge rectifiers in 100MHz and 2.4GHz bands,” *IEEE Wirel. Power Transf. Conf. 2014, IEEE WPTC 2014*, pp. 64–67, 2014.
- [16] J. H. Chou, D. B. Lin, K. L. Weng, and H. J. Li, “All polarization receiving rectenna with harmonic rejection property for wireless power transmission,” *IEEE Trans. Antennas Propag.*, vol. 62, no. 10, pp. 5242–5249, 2014.
- [17] M. H. Ouda, P. Mitcheson, and B. Clerckx, “Robust Wireless Power Receiver for Multi-Tone Waveforms,” *2019 49th Eur. Microw. Conf. EuMC 2019*, pp. 101–104, 2019.
- [18] C. Song, Y. Huang, J. Zhou, J. Zhang, S. Yuan, and P. Carter, “A high-efficiency broadband rectenna for ambient wireless energy harvesting,” *IEEE Trans. Antennas Propag.*, vol. 63, no. 8, pp. 3486–3495, 2015.

- [19] F. Bolos, J. Blanco, A. Collado, and A. Georgiadis, "RF Energy Harvesting from Multi-Tone and Digitally Modulated Signals," *IEEE Trans. Microw. Theory Tech.*, vol. 64, no. 6, pp. 1918–1927, Jun. 2016.
- [20] A. Quddious, M. A. Antoniadis, P. Vryonides, and S. Nikolaou, "Voltage-Doubler RF-to-DC Rectifiers for Ambient RF Energy Harvesting and Wireless Power Transfer Systems," *Recent Wirel. Power Transf. Technol.*, pp. 1–19, 2020.
- [21] A. Collado and A. Georgiadis, "Optimal waveforms for efficient wireless power transmission," *IEEE Microw. Wirel. Components Lett.*, vol. 24, no. 5, pp. 354–356, 2014.
- [22] S. A. Rotenberg, S. K. Podilchak, P. D. H. Re, C. Mateo-Segura, G. Goussetis, and J. Lee, "Efficient Rectifier for Wireless Power Transmission Systems," *IEEE Trans. Microw. Theory Tech.*, vol. 68, no. 5, pp. 1921–1932, 2020.
- [23] M. Terauds, L. Malbranque, and V. Smolaninovs, "Application of LoRaWAN for Interactive E-ink Based Schedule Board," in *2020 IEEE Microwave Theory and Techniques in Wireless Communications (MTTW)*, 2020, pp. 222–226.
- [24] A. Collado and A. Georgiadis, "Improving wireless power transmission efficiency using chaotic waveforms," *IEEE MTT-S Int. Microw. Symp. Dig.*, pp. 1–3, 2012.
- [25] A. Litvinenko, J. Eidaks, S. Tjukovs, D. Pikulins, and A. Aboltins, "Experimental Study of the Impact of Waveforms on the Efficiency of RF-to-DC Conversion Using a Classical Voltage Doubler Circuit," in *2018 Advances in Wireless and Optical Communications (RTUWO)*, 2018, pp. 257–262.
- [26] A. Litvinenko, J. Eidaks, and A. Aboltins, "Usage of signals with a high PAPR level for efficient wireless power transfer," *2018 IEEE 6th Work. Adv. Information, Electron. Electr. Eng. AIEEE 2018 – Proc.*, pp. 5–9, 2018.
- [27] J. Eidaks, A. Litvinenko, A. Aboltins, and D. Pikulins, "Signal Waveform Impact on Efficiency of Low Power Harvesting Devices in WSN," *Proc. 2019 IEEE Microw. Theory Tech. Wirel. Commun. MTTW 2019*, vol. 1, pp. 57–61, 2019.
- [28] J. Eidaks, A. Litvinenko, J. P. Chiriyankandath, M. A. Varghese, D. D. Shah, and Y. K. T. Prathakota, "Impact of signal waveform on RF-harvesting device performance in wireless sensor network," *2019 IEEE 60th Annu. Int. Sci. Conf. Power Electr. Eng. Riga Tech. Univ. RTUCON 2019 – Proc.*, 2019.
- [29] J. Eidaks, A. Litvinenko, A. Aboltins, and D. Pikulins, "Waveform Impact on Wireless Power Transfer Efficiency using Low-Power Harvesting Devices," *Electr. Control Commun. Eng.*, vol. 15, no. 2, pp. 96–103, 2019.
- [30] K. Mitani, Y. Kawamura, W. Kitagawa, and T. Takeshita, "Circuit modeling for common mode noise on AC/DC converter using sic device," *2019 21st Eur. Conf. Power Electron. Appl. EPE 2019 ECCE Eur.*, pp. 1–10, 2019.
- [31] D. Pikulin, "Complete bifurcation analysis of DC-DC converters under current mode control," *J. Phys. Conf. Ser.*, vol. 482, no. 1, 2014.
- [32] D. Pikulins, "Exploring types of instabilities in switching power converters: The complete bifurcation analysis," *Elektron. ir Elektrotechnika*, vol. 20, no. 5, pp. 76–79, 2014.
- [33] D. O. Pederson, "A historical review of circuit simulation," *IEEE Solid-State Circuits Mag.*, vol. 3, no. 2, pp. 43–54, 2011.
- [34] H. Liu and N. Wong, "Autonomous volterra algorithm for steady-state analysis of nonlinear circuits," *IEEE Trans. Comput. Des. Integr. Circuits Syst.*, vol. 32, no. 6, pp. 858–868, 2013.
- [35] G. De Luca, P. Bolcato, and W. H. A. Schilders, "Proper initial solution to start periodic steady-state-based methods," *IEEE Trans. Circuits Syst. I Regul. Pap.*, vol. 66, no. 3, pp. 1104–1115, 2019.
- [36] X. Y. Z. Xiong, L. J. Jiang, J. E. Schutt-Aine, and W. C. Chew, "Volterra Series-Based

- Time-Domain Macromodeling of Nonlinear Circuits,” *IEEE Trans. Components, Packag. Manuf. Technol.*, vol. 7, no. 1, pp. 39–49, 2017.
- [37] N. N. Krylov, N.N.B.; Krylov, N.N.; Bogoliubov, *Introduction to Nonlinear Mechanics*. NJ, USA: Princeton University Press: Princeton, 1995.
- [38] E. M. Baily, *Steady-State Harmonic Analysis of Non-Linear Networks*. Stanford, CA, USA: Stanford University: , USA, 1968.
- [39] Q.-J. Zhang, E. Gad, B. Nouri, W. Na, and M. Nakhla, “Simulation and Automated Modeling of Microwave Circuits: State-of-the-Art and Emerging Trends,” *IEEE J. Microwaves*, vol. 1, no. 1, pp. 494–507, 2021.
- [40] M. S. Nakhla and J. Vlach, “A Piecewise Harmonic Balance Technique for Determination of Periodic Response of Nonlinear Systems,” *IEEE Trans. Circuits Syst.*, vol. 23, no. 2, pp. 85–91, 1976.
- [41] S. Egami, “Nonlinear, Linear Analysis and Computer-Aided Design of Resistive Mixers,” *IEEE Trans. Microw. Theory Tech.*, vol. 22, no. 3, pp. 270–275, 1974.
- [42] A. R. Kerr, “A Technique for Determining the Local Oscillator Waveforms in a Microwave Mixer,” *IEEE Trans. Microw. Theory Tech.*, vol. 23, no. 10, pp. 828–831, 1975.
- [43] R. G. Hicks and P. J. Khan, “Numerical Analysis of Nonlinear Solid-State Device Excitation in Microwave Circuits,” *IEEE Trans. Microw. Theory Tech.*, vol. 30, no. 3, pp. 251–259, 1982.
- [44] F. Filicori, M. R. Scalas, and C. Naldi, “Nonlinear circuit analysis through periodic spline approximation,” *Electron. Lett.*, vol. 15, no. 19, p. 597, 1979.
- [45] P. D. Cooley, J.W.; Lewis, P.A.W.; Welch, *The Fast Fourier Transform and Its Applications*. IEEE Trans. Educ., 1969.
- [46] M. B. Gilmore, R.J.; Steer2, *Nonlinear Circuit Analysis Using the Method of Harmonic Balance-A Review of the Art. Part I. Introductory Concepts*. Int. J. Microw. Millim. Wave Comput. Aided Eng., 1991.
- [47] V. Rizzoli, A. Lippardini, and E. Marazzi, “A General-Purpose Program for Nonlinear Microwave Circuit Design,” *IEEE Trans. Microw. Theory Tech.*, vol. 31, no. 9, pp. 762–770, 1983.
- [48] R. J. Gutmann and J. M. Borrego, “Power Combining in an Array of Microwave Power Rectifiers,” in *MTT-S International Microwave Symposium Digest*, vol. 79, pp. 453–455.
- [49] Jiapin Guo and Xinen Zhu, “An improved analytical model for RF-DC conversion efficiency in microwave rectifiers,” in *2012 IEEE/MTT-S International Microwave Symposium Digest*, 2012, pp. 1–3.
- [50] J. Guo, H. Zhang, and X. Zhu, “Theoretical Analysis of RF-DC Conversion Efficiency for Class-F Rectifiers,” *IEEE Trans. Microw. Theory Tech.*, vol. 62, no. 4, pp. 977–985, Apr. 2014.
- [51] T. Hirakawa and N. Shinohara, “Theoretical Analysis and Novel Simulation for Single Shunt Rectifiers,” *IEEE Access*, vol. 9, pp. 16615–16622, 2021.
- [52] N. Pan, D. Belo, M. Rajabi, D. Schreurs, N. B. Carvalho, and S. Pollin, “Bandwidth Analysis of RF-DC Converters Under Multisine Excitation,” *IEEE Trans. Microw. Theory Tech.*, vol. 66, no. 2, pp. 791–802, Feb. 2018.
- [53] T. Ohira, “Power efficiency and optimum load formulas on RF rectifiers featuring flow-angle equations,” *IEICE Electron. Express*, vol. 10, no. 11, pp. 20130230–20130230, 2013.
- [54] S. Hageman, “What PCB material do I need to use for RF?,” *What PCB material do I need to use for RF?* [Online]. Available: <https://www.edn.com/what-pcb-material-do-i-need-to-use-for-rf/>.
- [55] ROGERS CORPORATION, “RO4000 Series High Frequency Circuit Materials,” 2018.

- [Online]. Available: <https://rogerscorp.com/-/media/project/rogerscorp/documents/advanced-electronics-solutions/english/data-sheets/ro4000-laminates-ro4003c-and-ro4350b---data-sheet.pdf>.
- [56] “Silicon Schottky Diode: BAT63,” 2003. [Online]. Available: https://www.infineon.com/dgdl/Infineon-BAT63SERIES-DS-v01_01-en.pdf?fileId=db3a304314dca38901151817843c0df4.
- [57] Skyworks Solutions, “Surface Mount Mixer and Detector Schottky Diodes,” *Datasheet*, 2018. [Online]. Available: <https://www.skyworksinc.com/Products/Diodes/SMS7621-Series>.
- [58] “HSMS-285x Series Datasheet,” *HSMS-285x Series Datasheet*. [Online]. Available: <https://www.broadcom.com/products/wireless/diodes/schottky/hsms-285c>. [Accessed: 30-Aug-2018].
- [59] A. Litvinenko, R. Kusnins, A. Aboltins, J. Eidaks, D. Laksis, and J. Sadovksis, “About Simultaneous Information and Power Transfer in WSN using Frequency Modulation,” in *2020 IEEE 8th Workshop on Advances in Information, Electronic and Electrical Engineering, AIEEE 2020 - Proceedings*, 2021.
- [60] A. Litvinenko, R. Kusnins, A. Aboltins, J. Eidaks, D. Laksis, and J. Sadovksis, “About Simultaneous Information and Power Transfer in WSN using Frequency Modulation,” *2020 IEEE 8th Work. Adv. Information, Electron. Electr. Eng. AIEEE 2020 - Proc.*, 2021.



Jānis Eidaks was born in 1993 in Balvi. He received his Bachelor's degree of Science in Electrical Engineering in 2015 and a Master's degree in Electronics in 2017 from Riga Technical University. From 2016 to 2018 he worked in the Quality Assurance Department of LEXEL FABRIKA. Since 2017, he has been an assistant and scientific assistant with the Faculty of Electronics and Telecommunications, since 2022 he works as information technology administrator in HPC Center. His research interests include development of autonomous powering solutions and low power sensor network nodes.